P-05-156

Forsmark site investigation

Petrographic and geochemical characteristics of bedrock samples from boreholes KFM04A–06A, and a whitened alteration rock

Jesper Petersson, Johan Berglund,
Peter Danielsson, Göran Skogsmo
SwedPower AB

May 2005

Svensk Kärnbränslehantering AB
Swedish Nuclear Fuel
and Waste Management Co
Box 5864
SE-102 40 Stockholm Sweden
Tel 08-459 84 00
+46 8 459 84 00
Fax 08-661 57 19
+46 8 661 57 19

ISSN 1651-4416
SKB P-05-156

Forsmark site investigation

Petrographic and geochemical characteristics of bedrock samples from boreholes KFM04A–06A, and a whitened alteration rock

Jesper Petersson, Johan Berglund,
Peter Danielsson, Göran Skogsmo
SwedPower AB

May 2005

Keywords: KFM04A, KFM05A, KFM06A, Geology, Alteration, Petrography, Geochemistry, Forsmark, AP PF 400-04-124.

Abstract

This report presents petrographic and geochemical data for rock samples from the telescopic boreholes KFM04A, KFM05A and KFM06A drilled in the northern part of the Forsmark candidate area. The study aims to give a systematic documentation of rock units and features of petrographic interest in the three boreholes, with special attention to a whitened alteration rock encountered in the lower part of KFM06A. The analytical programme included whole-rock geochemical analysis, as well as optical examination and modal analysis of thin-sections, complemented by EDS-analysis of feldspars in the whitened alteration rock and its unaltered equivalents.

The overall structure of the report is based on a few specific questions from each borehole, and includes the following rocks: (1) various rock units in the ductile, high-strain boundary in the upper half of KFM04A, (2) a fine- to finely medium-grained facies of a typically medium-grained metagranite-granodiorite in KFM05A, (3) a whitened alteration rock in the lower part of KFM06A, which also occurs in outcrops along the northeastern margin of the candidate area, and (4) amphibolites and related rocks in KFM04A and KFM05A. Although the report is largely descriptive, there are sections that are more interpretative, particularly that of the whitened alteration rock.

Since the rock volume affected by the whitish alteration is significant along the north-eastern margin of the candidate area, it required special attention. According to both the mineralogical and geochemical classification, the affected rocks are presently tonalites, composed of 90–95 vol. % plagioclase and quartz. Microscopic examination reveals a typically metamorphic texture without any distinguishable zonation or rimming of the plagioclase. The alteration is, therefore, inferred to be pre- or possibly syn-metamorphic. The anorthite content in the plagioclase observed in the whitened alteration rock, is lower than in plagioclase in the unaltered wall rock. This, in addition to the exceedingly low content of K-feldspar, suggests that the alteration is a form of albitization, and that the present mineralogy and composition of the feldspars is a result of metamorphic alkali redistribution. Another important result, as indicated by varying distribution and composition of the ferromagnesian assemblages among the samples, is that more than one rock type was affected by the alteration. Finally, the whitened alteration rock exhibits an enrichment of typically immobile trace elements, suggesting that the rock was subjected to volume reduction and/or mass loss.

Sammanfattning

Föreliggande rapport redovisar petrografisk och geokemisk data för ett antal bergartsprover från teleskopborrhål KFM04A–6A i norra delen av Forsmarksområdet. Undersökningen syftar till att ge en systematisk dokumentation av bergartsenheter och företeelser av petrografiskt intresse i de tre borrhålen, med speciell fokus på en vitfärgad omvandlingsbergart som påträffats i undre delen av KFM06A. Analysprogrammet omfattar geokemisk bergartsanalys, samt optisk granskning och modalanalys av tunnslip, kompletterat med EDS-analyser av fältspat i den vitfärgade omvandlingsbergarten och dess oomvandlade motsvarigheter.

Rapportens övergripande struktur baserar sig på ett fåtal specifika frågeställningar i varje borrhål och inkluderar följande bergarter: (1) olika bergartsenheter i den kraftigt plastiskt deformerade övre delen av KFM04A, (2) en fin- till fint medelkornig variant av en normalt medelkornig metagranit-granodiorit i KFM05A, (3) en vitfärgad omvandlingsbergart i den undre delen av KFM06A, som också förekommer i hällar längs den nordöstra begränsningen av kandidatområdet, och (4) amfiboliter och liknande bergarter i KFM04A och KFM05A. Trots att rapporten generellt är deskriptiv, finns det delar med mer långtgående tolkningar, speciellt de som behandlar den vitfärgade omvandlingsbergarten.

Eftersom bergartsvolymen som påverkats av den vitfärgade omvandlingen är betydande längs den nordöstra begränsningen av kandidatområdet, har studien främst fokuserats på denna. Enligt både den mineralogiska och geokemiska klassificeringen är de påverkade bergarterna tonaliter, bestående av 90–95 vol. % plagioklas och kvarts. Mikroskopering avslöjar en typisk metamorf bergartstextur utan någon urskiljbar zonering eller liknande i plagioklasen. Omvandlingen får därför anses vara pre- eller möjligtvis syn-metamorf. Anortit-innehållet i plagioklas från omvandlingsbergarten är därtill lägre än i plagioklas från det opåverkade sidoberget. Detta, liksom det mycket låga innehållet av K-fältspat, indikerar att omvandlingen är en form av albitisering, och att den nuvarande mineralogin och fältspaternas sammansättning är ett resultat av metamorf alkaliomfördelning. En annan viktig slutsats som indikeras av variationer i fördelning och förekomst av järn-magnesium-bärande mineral bland proverna är att mer än en bergart har genomgått omvandling. Slutligen är den vitfärgade omvandlingsbergarten anrikad på spårelement som normalt brukar betraktas vara immobila, vilket indikerar att bergarten genomgått volymminskning och/eller massförlust.

Contents

1 Introduction

Since 2002, SKB investigates two potential sites at Forsmark and Oskarshamn for a deep repository in the Swedish Precambrian basement. In order to characterise the bedrock down to a depth of about 1 km in the central part of the candidate area at Forsmark, three deep telescopic boreholes were drilled. Each borehole starts with 100 m of percussion drilling, followed by core drilling down to about 1,000 m depth. After completion of these initial drillings, SKB launched a more extensive, complementary drilling programme, aiming to solve more specific geological questions. The investigations were concentrated to the northern part of the candidate area, and the first of these boreholes, KFM04A, probes the north-western boundary of the tectonic lens, which defines the test site area (i.e. rock domain 029; see /SKB, 2004/). Two additional boreholes, KFM05A and KFM06A, were drilled in the area to investigate the existence of N–S and NE–SW trending deformation zones. During this work, a major occurrence of whitened alteration rock was encountered in the lower part of KFM06A. Surface exposures of similar rock types are known from the field investigations along the north-eastern margin of the tectonic lens, carried out by the SGU during 2002 and 2003. Since the rock volume affected by this alteration appears to be significant in certain parts of the area, it was judged necessary to initiate a more systematic study. Apart from this, the boreholes KFM04A and KFM05A revealed several additional rock units that merit thorough study. In borehole KFM04A, these primarily include the main rock types of the ductile, high-strain belt, which defines the southwestern boundary of the tectonic lens (Figure 1-1). Another important rock type found in borehole KFM05A is a more fine-grained variety of the prevalent metagranite-granodiorite in the tectonic lens. In addition, there are a number of less conspicuous, but yet anomalous, occurrences that require special attention.

In order to obtain a compositional documentation of these rock units, a project involving petrographic and geochemical analyses was initiated by SKB during October 2004. The analytical programme includes mainly optical examination of thin-sections and geochemical analysis of whole-rock samples. However, the study of the whitened alteration rock found within borehole KFM06A and in outcrops along the northeastern margin of the candidate area was also complemented by EDS-analysis of feldspars.

The purpose of this report is to present the results from the petrographic and geochemical study of samples from boreholes KFM04A–6A, as well as a few surface samples of the whitened alteration rock, collected by the SGU during their field investigations. Although the report is largely descriptive, it has proved impossible to omit discussion in some cases, particularly with the whitened alteration rock where petrography and feldspar composition goes hand in hand with an interpretation of its origin. A more in-depth discussion is, however, beyond the scope of this study. To facilitate comparison with corresponding data for samples from the surface bedrock mapping and the pervious three cored boreholes (KFM01A–03A), the choice of diagrams for data presentation, etc follows that of /Stephens et al. 2003; Petersson et al. 2004c/. The work was carried out in accordance with the activity plan AP PF 400-04-124. In Table 1-1 controlling documents for performing this activity are listed. Both activity plan and method description are part of SKB's internal controlling documents.

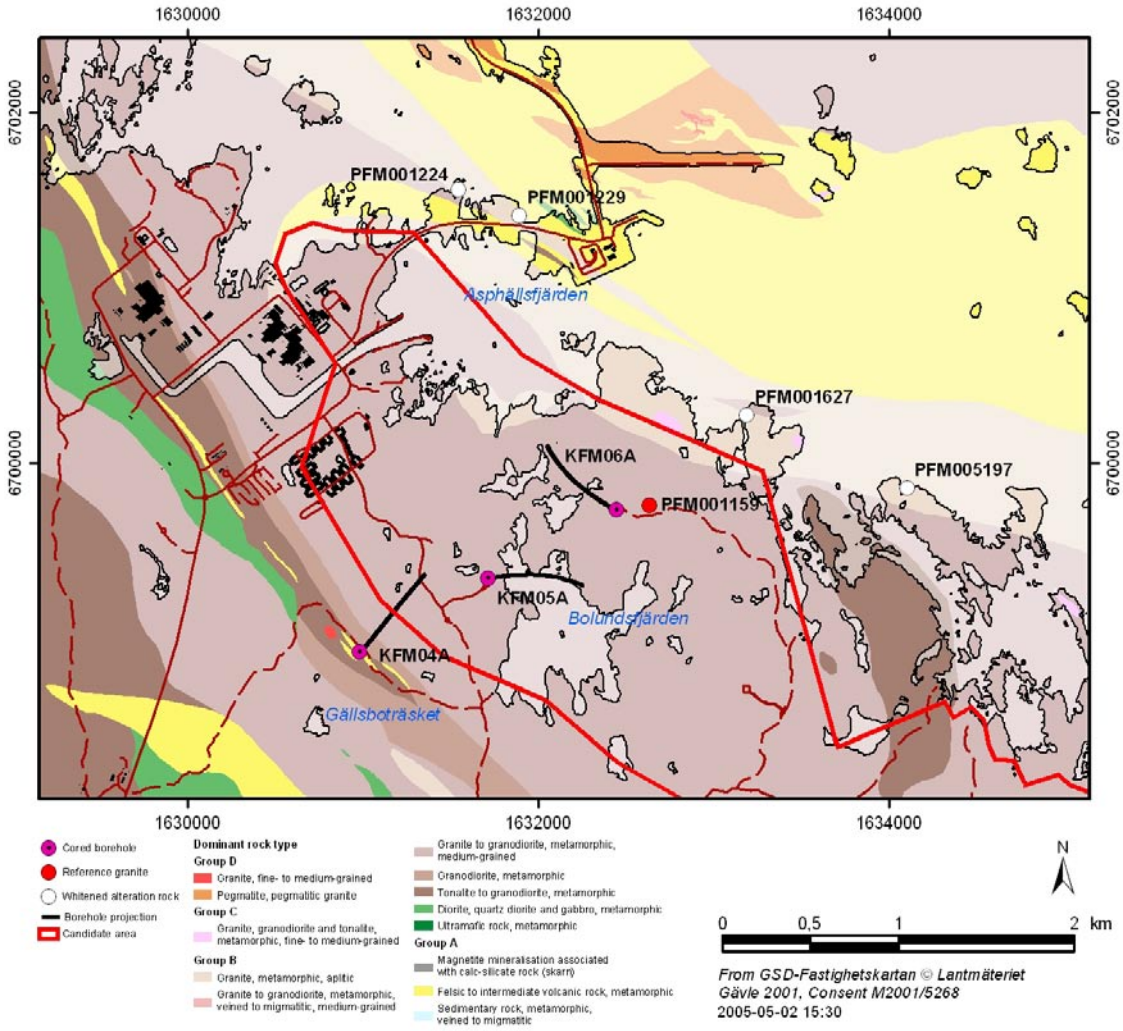

Figure 1-1. *Generalized geological map over the northern part of Forsmark site investigation area showing projections of cored boreholes KFM04A, KFM05A and KFM06A, and selected outcrop samples (PFM).*

Table 1-1. Controlling documents for the performance of the activity.

Activity plan	**Number**	**Version**
Geokemisk, petrografisk och mineralogisk analys av bergartsprov från KFM04A, KFM05A och KFM06A	AP PF 400-04-124	1.0
Method documents	**Number**	**Version**
Metodbeskrivning för bergartsanalyser	SKB MD 160.001	1.0

2 Objective and scope

The present work was undertaken to obtain (1) petrographic and geochemical whole-rock data for a number of rock units within the boreholes KFM04A–06A, and (2) EDS-analyses of feldspars from the whitened alteration rock found in KFM06A and outcrops along the northeastern margin of the candidate area, as well as its apparently unaltered equivalence. The main objective of the project has been to gain a better understanding of the nature and origin of these rocks, with special attention to the whitened alteration rock. This in turn is essential for the forthcoming three-dimensional, descriptive modelling of the area.

A summary of all thin-sections and whole-rock geochemical samples from the three boreholes are given in Table 2-1. Totally, 19 samples were collected for thin-section preparation. Fifteen of these underwent modal analysis. Samples for whole-rock geochemical analysis were taken adjacent to all of the modally analysed thin-sections. The four thin-sections that lack modal analysis were all collected to give answer to specific petrographic questions.

Also included in Table 2-1 are five samples collected by the SGU during their field investigation in the area. Four of them represent different varieties of the whitened alteration rock, whereas the fifth is apparently unaffected reference granite. Thin-sections of these samples were used for complementary EDS-analysis of feldspars. The presentations of the whole-rock geochemical and modal analyses for these samples are here limited to various diagrams and the complete analyses can be found in a separate report by /Stephens et al. 2005/.

Table 2-1. Compilation of all thin-sections and geochemical samples analysed from boreholes KFM04A–6A. Also included are the five samples collected by the SGU during their field investigation in the area. Macroscopic character and rock classification based on macroscopic, modal and chemical classification are given when available.

Core	Sampled core section		Rock	Rock classification			Macroscopic character		
	Thin section	Geochemistry	group	Macroscopic	Modal	Chemical (QP)	Colour	Structure	Other
KFM04A	117.70–117.74	116.51–116.70	**B**	Metagranodiorite	Granodiorite	Tonalite	Dark grey	Strong foliation	–
	124.56–124.60	124.60–124.80	**A**	Intermediate metavolcanite	Dacite	Dacite	Dark grey	Weak foliation	–
	186.65–186.70	186.57–186.80	**B**	Metagranite-granodiorite	Monzogranite	Adamellite	Reddish grey	Strong foliation	–
	271.40–271.44	271.64–271.84	**B**	Metagranite-granodiorite	Granodiorite	Adamellite	Reddish grey	Strong foliation	–
	400.96–401.04*	–	**B**	Muscovite altered DZ	–	–	Grey	Strong foliation	Ductile deformation zone
	446.08–446.12*	–	**B**	Amphibolite	–	–	Dark grey	–	–
	737.61–737.65	737.41–737.61	**B**	Amphibolite	Quartz diorite	Quartz diorite	Dark grey	Weak foliation	–
KFM05A	807.96–808.00*	–	**B**	Intermediate metavolcanite	–	–	Dark grey	Weak foliation	–
	152.66–152.70	152.46–152.66	**B**	Metagranite-granodiorite	Monzogranite	Granodiorite	Reddish grey	Mineral lineation	Fine- to medium-grained
	272.11–272.15	271.90–272.11	**B**	Metagranite-granodiorite	Monzogranite	Adamellite	Reddish grey	Weak foliation	Fine- to medium-grained
	285.74–285.81*	–	**B**	Metagranite-granodiorite	–	–	Reddish grey	Weak foliation	Contact between metagranites
	299.19–299.23	298.82–299.02	**B**	Metagranite-granodiorite	Granodiorite	Granodiorite	Reddish grey	Faint foliation	–
	356.07–356.11	355.87–356.07	**B**	Amphibolite	Gabbro/diorite	Gabbro/diorite	Dark grey	–	Heterogeneous
KFM06A	691.78–691.82	691.58–691.78	**C**	Metagranitoid	Granodiorite	Tonalite	Grey	–	–
	636.34–636.37	636.14–636.34	**B**	Aplitic metagranite	Monzogranite	Adamellite	Reddish grey	Mineral lineation	Fine-grained
	757.48–757.52	756.82–757.02	**B**	Metagranite-granodiorite	Tonalite	Tonalite	Light grey	Mineral lineation	Whitened and strongly altered
	818.33–818.36	818.42–818.62	**B**	Aplitic metagranite	Tonalite	Tonalite	Light grey	Foliation/Banding	Whitened and strongly altered
	850.79–850.82	850.59–850.79	**B**	Aplitic metagranite	Tonalite	Tonalite	Light grey	Mineral lineation	Whitened and strongly altered
	937.95–937.99	937.75–937.95	**B**	Aplitic metagranite	Tonalite	Tonalite	Light grey	Lineation/Foliation	Whitened and strongly altered
Outcrop samples									
PFM001159B			**B**	Metagranite-granodiorite	Monzogranite	Adamellite	Greyish red	Medium foliation	Reference granite
PFM001224B			**B**	Metagranite-granodiorite	Tonalite	Tonalite	Grey	Medium foliation	Whitened and strongly altered
PFM001229B			**B**	Metagranite-granodiorite	Tonalite	Tonalite	Light grey	Mineral lineation	Whitened and altered
PFM001627A			**B**	Aplitic metagranite	Tonalite	Tonalite	Reddish grey	Medium foliation	Slightly whitened and altered
PFM005197A			**B**	Metagranite-granodiorite	Granodiorite	Tonalite	Reddish grey	Medium foliation	Slightly whitened and altered

*No modal analysis.

3 Equipment

Optical microscopic investigations and modal analysis were carried out at the at Earth Sciences Centre, Göteborg University, using standard polarizing microscopes with attached point counter equipment. Photomicrographs were taken using a polarizing microscope with digital photographic equipment at the SGU in Göteborg.

Core samples selected for whole-rock geochemical analysis and gamma-ray spectrometry were prepared for analysis by crushing and pulverizing at Swedish Geochem Services AB, Öjebyn. The samples were crushed using a Mn-steel crusher and pulverized using a LM5 mill. The powdered samples were subsequently analysed geochemically at the Acme Analytical Laboratories Ltd in Vancouver, Canada using the ICP (Inductively Coupled Plasma) technique. This laboratory was satisfactorily accredited under ISO 9002 during November 1996.

Mineral identification and semi-quantitative feldspar analysis were made using a Link® energy-dispersive spectrometer (EDS) attached to a Zeiss®DSM 940 scanning electron microscope (SEM) at Earth Sciences Centre, Göteborg University.

4 Execution

4.1 General

The sample preparation, the analytical work and the data handling have followed the procedures recommended in the description of the methods for the analyses of bedrock samples (SKB MD 160.001; SKB internal controlling document).

Information regarding the methodology of modal and whole-rock geochemical analysis of the five outcrop samples is given in a separate report for the bedrock mapping by /Stephens et al. 2005/.

4.2 Perparatory work

Polished thin-sections, from up to 4 cm long core sections, were prepared by Minoprep in Hunnebostrand. About 20 cm long, splited core samples, selected for whole-rock geochemical analysis (weighing 0.5–0.6 kg), were crushed and pulverized by Swedish Geochem Services AB. Crushing to a size of < 10 mm in a Mn-steel crusher was followed by grinding to a powder with a size of < 200 mesh (90%) in a LM5 mill. The procedure is estimated to give rise to minor contamination of the elements Fe (~600 ppm), Mn (~9 ppm) and Cr (~1.5 ppm).

4.3 Analytical work

All modal analysis were done by Jesper Petersson (SwedPower AB) by determining the mineral composition at 500 evenly spaced points over each thin-section. In order to estimate the reproducibility of the modal data, one of the thin-sections (636.34–636.37 m in KFM06A) was analyzed by two geologists: Thomas Eliasson, SGU, and Jesper Petersson. Most strikingly, the K-feldspar content differs by 8 vol. % between the two counting series (cf Appendix 2). This may, of course, be due to problems in the distinction between K-feldspar and plagioclase. However, also the biotite content differs markedly by being 6.9 and 10.2 vol. %, respectively. This suggests that the differences mainly can be ascribed to textural heterogeneities in the rock. Therefore, some samples might have too coarse mineral domains to give reliable mineral modes by conventional point counting. In addition to point counting, the grain-size as well as the relevant textural and micro-structural characteristics of each sample was documented (Appendix 1). However, three of the thin-sections from KFM04A were collected to give answers to petrographic questions where modal analysis is irrelevant, and they were therefore only analyzed qualitatively.

Whole-rock geochemical analyses were carried out by Acme Analytical Laboratories Ltd in Vancouver, Canada. The samples were sent for analysis in two separate batches; data for KFM04A and KFM05A were delivered at 2004-12-23 (File # A407315), whereas the data for KFM06A were delivered at 2005-03-01 (File # A500575). All major and minor oxides (SiO_2, Al_2O_3, Fe_2O_3, MgO, CaO, Na_2O, K_2O, TiO_2, P_2O_5, and MnO) and some trace element compositions (Sc, Cr, Ni and Ba) were analysed by ICP-AES, C and S by the Leco method and the trace elements V, Co, Cu, Zn, Ga, As, Rb, Sr, Y, Zr, Nb, Mo, Ag, Cd, Sn, Sb, Cs, Hf, Ta, W, Au, Hg, Tl, Pb, Bi, Th, U and the REE by ICP-MS. A more detailed

description of the methodology is given by /Stephens et al. 2003/. Duplicate analysis of sample 317.05–317.45 from KFM02A showed that the reproducibility is better than about 25% for concentrations up to ten times the detection limit, 10% for concentrations up to 50 times the detection limit and better than 7% for higher concentrations.

EDS analysis were carried out on feldspars in nine thin-sections under the following operating conditions: acceleration voltage 25 kV, measured beam current c 1 nA and counting live-time of 100 s. A general spot size of c 1 μm was used. The routine analytical set-up covers the elements Si, Ti, Al, Fe, Mg, Na, Ca and K. A Co-standard was used as reference to monitor the instrument drift. The equipment utilizes Link's software for ZAF-correction and data processing, with natural and synthetic mineral standards. Iron is assumed to be ferrous in these calculations. The general detection limit is as follows: 0.1% for SiO_2, 0.02% for TiO_2, 0.03% for Al_2O_3, 0.05% for FeO, 0.04% for MgO, 0.3% for Na_2O, 0.05% for CaO and 0.1% for K2O.

4.4 Data handling

The data from this activity are stored in the SICADA database and are traceable by the activity plan number.

5 Results

5.1 General

Based on the field mapping of bedrock outcrops in the Forsmark area, /Stephens et al. 2003/ defined four major rock groups, designated A, B, C and D. All previous presentations of petrographic and geochemical data from the Forsmark area rest on this division. However, the alphabetical designations relate more or less entirely to the temporal relationship between the lithologies; a rather marginal issue in the present report, which mainly focuses on geological problems of more local character. The overall structure of this chapter is, therefore, based on a few specific questions from each borehole, and all samples are discussed in terms of the bedrock nomenclature defined by SKB. The alphabetical designations are nevertheless included in some figures and tables to facilitate comparison with corresponding data for surface and borehole samples from /Stephens et al. 2003; Petersson et al. 2004c/.

The petrographic account as follows for the various rock types in this chapter is a condensed version of the observations presented for individual thin-section in Appendix 1. Modal analyses for most of those thin-sections are listed in Appendix 2. Major and trace element compositions of the samples are listed in Appendix 3.

Except for the two amphibolite samples, all rocks analysed modally are quartz-rich metagranitoids that form two rather distinct groupings in a QAP classification diagram (Figure 5-1): samples mapped as metagranite-granodiorite (101057) fall all on or close to the boundary between the granite and granodiorite fields, whereas the remaining samples, including those of the whitened alteration rock, plot in the tonalite field or along the boundary between the granodiorite and tonalite fields. In the P-Q diagram of /Debon; LeFort, 1983/, this pattern becomes even more distinct (Figure 5-2). The main reason for this more limited variability within each rock group is that the apparent spread in quartz contents, as revealed by the modal analyses, is without parallel in the whole-rock silica content. This may, of course, be due to problems in the distinction between quartz and feldspars during the point counting analysis. An explanation, which is further supported by the fact that the analyses from /Stephens et al. 2005/ for the five outcrop samples, generally are lower in quartz than corresponding samples from the drill cores.

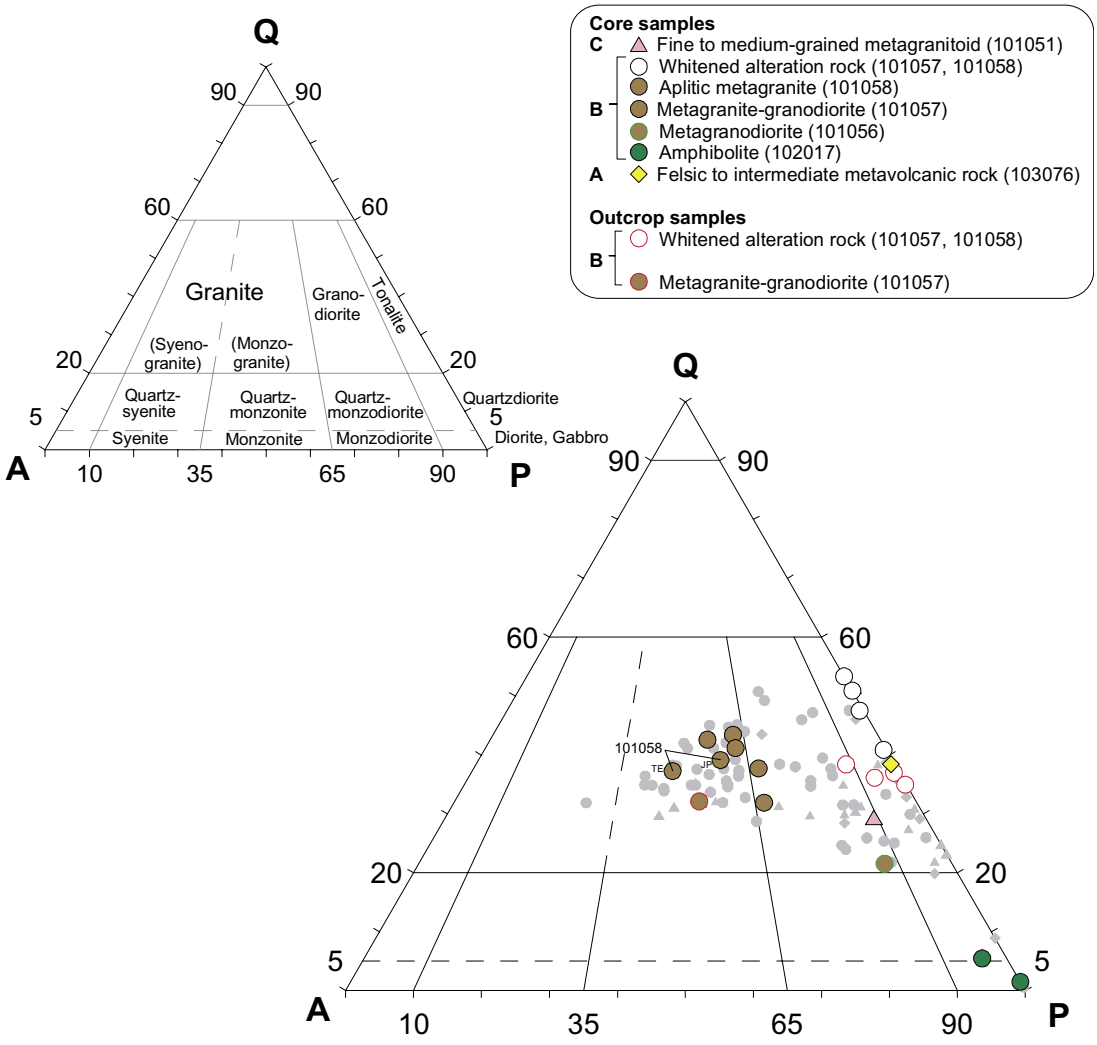

Figure 5-1. *Modal classification diagram after /Streckeisen, 1976/ for all rocks analysed in this study and the five outcrop samples from /Stephens et al. 2005/. Corresponding data for samples from the surface bedrock mapping and the previous three cored boreholes (KFM01A–03A) from /Stephens et al. 2003; Petersson et al. 2004c/ are included as shaded symbols for comparison.*

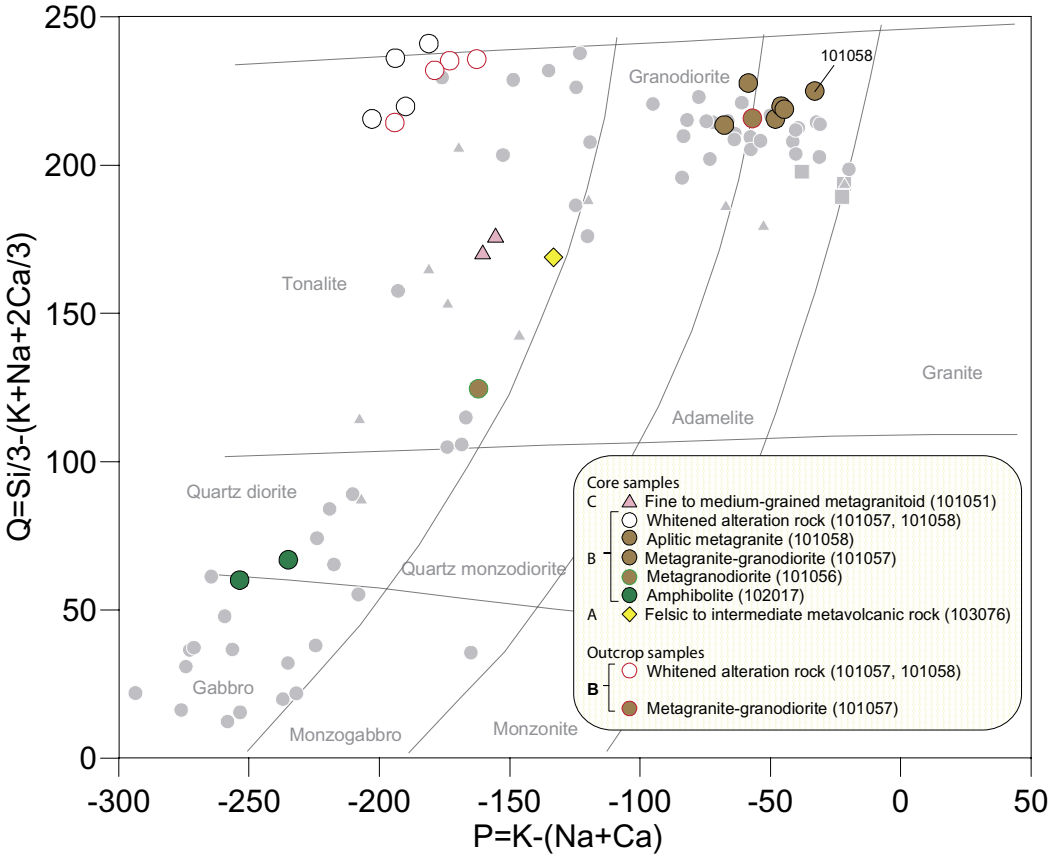

Figure 5-2. *Q-P diagram after /Debon and LeFort, 1983/ illustrating the compositional characteristics for all rocks analysed in this study and the five outcrop samples from /Stephens et al. 2005/. Corresponding data for samples from the surface bedrock mapping and the previous three cored boreholes (KFM01A–03A) from /Stephens et al. 2003; Petersson et al. 2004c/ are included as shaded symbols for comparison.*

5.2 The ductile, high-strain boundary in KFM04A

Borehole KFM04A was located in the ductile, high-strain belt, which defines the southwestern boundary of the test site area, and plunges 60 towards NE, into the tectonic lens. The upper part of the borehole, within the high-strain belt, is characterized by strong penetrative foliation, generally striking SE and dipping steeply towards SW cf /Petersson et al. 2004a/. Based on ocular inspection, the uppermost 176 metres of the borehole is dominated by a sequence of fine- to finely medium-grained metagranodiorite (rock code 101056) with occurrences of felsic to intermediate rocks of inferred volcanic origin (rock code 103076). Below 176 metres, the metagranodiorite becomes more granitic, and the rock is inferred to be a more strongly deformed variety of the medium-grained metagranite-granodiorite (rock code 101057), which is the dominating rock type of the tectonic lens. In some of the major ductile, high-strain zones in the borehole, there are two rather long sections of intense muscovitization (394.5–401.4 m and 426.2–430.6 m length) that renders recognition of the protoliths almost impossible.

5.2.1 Fine-grained, intermediate rock of inferred volcanic origin (103076)

Samples: *thin-section 124.56–124.60 m and whole-rock geochemical sample 124.60–124.80 m.*

Dark grey, equigranular rock with well-defined tectonic fabric. The grain-size is typically 0.2–0.6 mm and the fine-grained character is accentuated by a strikingly homogeneous distribution of the major components (i.e. no aggregation). Thus, apart from the grain-size, there are no textural or structural features that unambiguously support a volcanic origin. Both classification diagrams (Figures 5-1 and 5-2), as well as the macroscopic examination, reveal that the rock is dacitic, with plagioclase, quartz and biotite as the major constituents. Similar to some of the dacitic rocks of inferred volcanic origin in the area (e.g. PFM000352B and PFM001200A in /Stephens et al. 2003/), hornblende is notably absent. The retrogressive effects are limited to local sericitization of plagioclase and weak chloritization of biotite. The accessory assemblage includes K-feldspar, apatite, epidote, sphene (< 40 μm), allanite, zircon (< 20 μm) and hematite (< 20 μm).

The trace element composition of the rock is typical for granitoids with a general enrichment of large ion lithophile (LIL) elements and rare earth elements (REE) relative to high field strength (HFS) elements and heavy REE (Figure 5-3). However, a noteworthy feature is that the trace element composition is virtually identical to that of the surrounding metagranodiorite, as described in the following section. The only significant differences in the petrogenetic trace element patterns of Figure 5-3 are the magnitude of the Sr and Ti anomalies.

5.2.2 Strongly foliated metagranodiorite (101056) and metagranite-granodiotite (101057)

Samples: *thin-sections 117.70–117.74, 186.65–186.70 and 271.40–271.44 m and whole-rock geochemical samples 116.51–116.70, 186.57–186.80 and 271.64–271.84 m.*

One of the problems during the mapping of the upper, intensely deformed part of KFM04A was to separate the metagranodiorite (rock code 101056) that forms a continuous belt along the southwestern margin of the tectonic lens, from a texturally identical rock of more granitic composition, which is inferred to be a strongly deformed variety of the medium-grained metagranite-granodiorite (rock code 101057). The contact between the two units was located at a borehole length of 176 m. However, this is based on ocular estimates that remain to be verified by petrographic and geochemical analysis. For this purpose, we selected three samples, one from the inferred metagranodiorite and two from the more granitic variety.

The main macroscopic criterion for discrimination between the two rock varieties is their colour; the metagranite-granodiorite appears typically somewhat more light coloured and reddish than the metagranodiorite. Microscopic examination of the three samples reveals indeed considerable mineralogical differences between the two rock types. Most conspicuous is the modal content of ferromagnesian phases, which is 27.4 vol. % in the metagranodiorite and merely 6.6 vol. % in the two metagranite-granodiorite samples.

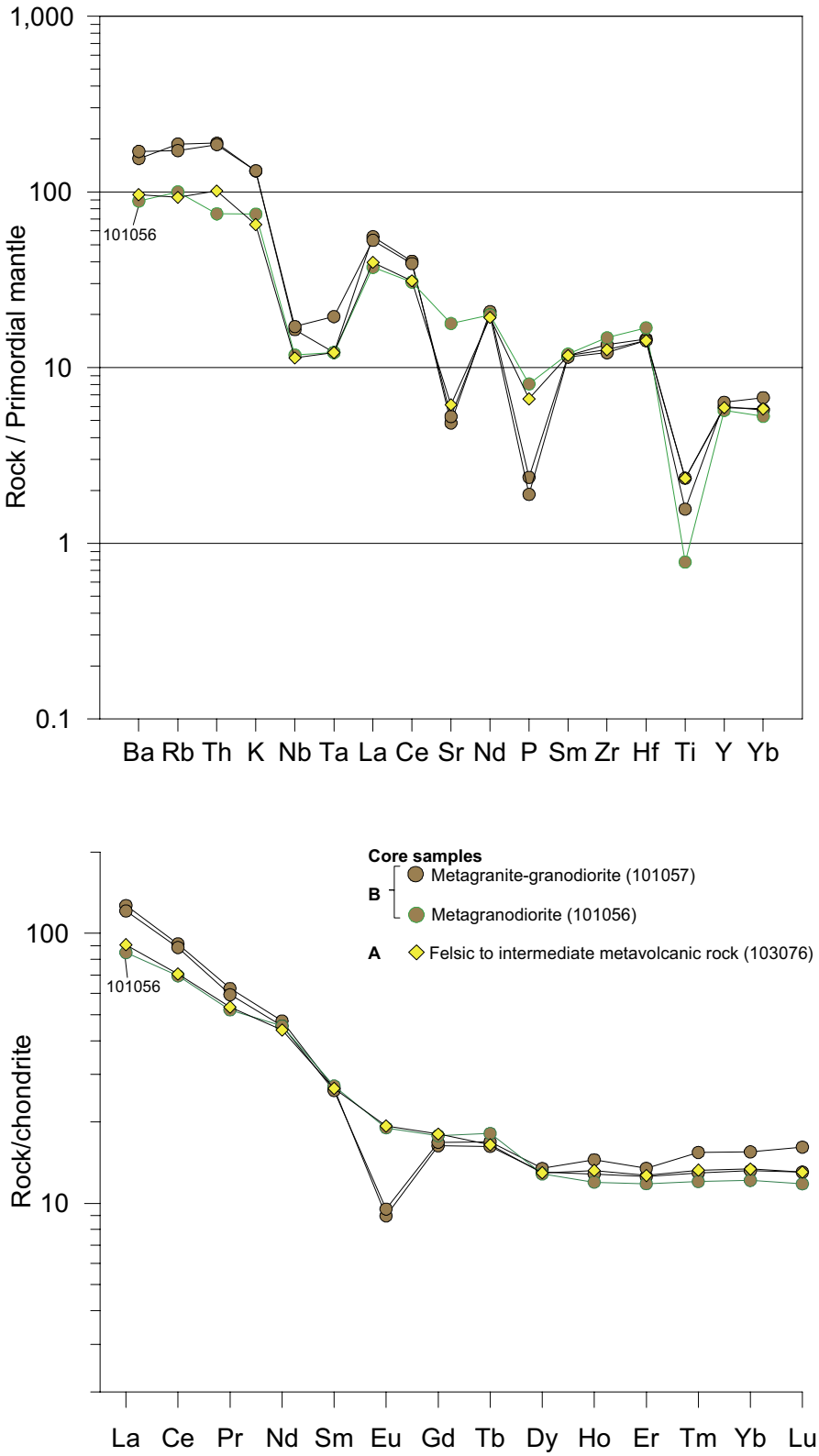

Figure 5-3. *Trace element variation diagrams for rocks from the ductile, high-strain boundary in KFM04A. The upper diagram shows the relationships between large ion lithophile (LIL) and high field strength (HFS) elements normalized to the composition of the primordial mantle, whereas the lower diagram shows the rare earth element abundances normalized to chondritic meteorite values. Primordial mantle values of 92.000 for P /Sun, 1980/ and 0.481 for Yb; all other after /McDonough et al. 1992/. Normalization factors for chondrite from /Boynton, 1984/.*

The ferromagnesian phases in the metagranodiorite includes, moreover, 16.2 vol. % hornblende, a mineral which is absent in the two metagranite-granodiorite samples. The differences are also evident in the QAP classification diagram (Figure 5-1) where the two samples mapped as metagranite-granodiorite plot close to the boundary between the monzogranite–granodiorite fields, whereas the inferred metagranodiorite sample falls in the lower right corner of the granodiorite field. However, the textural character of the two rock types is almost identical, and both shows a granular texture with irregular grain-boundaries and a distinct deformational fabric defined by elongated domains of feldspars, strained quartz and thin streaks of ferromagnesian phases. The general grain-size is less than 1 mm, with a few grains ranging up 1.5 mm. Also the texture and character of individual minerals are similar, though there are differences. Quartz is among the coarsest minerals within the two metagranite-granodiorite samples. In the metagranodiorite sample, on the other hand, it rarely exceeds 0.3 mm in size. Perthitic albite, which locally occurs as thin lamellae or 'flames' in K-feldspar from the metagranite-granodiorite appears to be absent in the metagranodiorite. The principal opaque mineral in the metagranite-granodiorite samples is magnetite, whereas only minor grains of pyrite were distinguished in the metagranodiorite.

The two rock types are also separable by their chemical composition, with a general agreement between the modal classification and the P-Q diagram (Figure 5-2). The less evolved character of the metagranodiorite relative to the metagranite-granodiorite is clearly reflected in the abundance of LIL and HFS elements (Figure 5-3). The metagranodiorite has, moreover, a lower total REE content, and its chondrite normalized REE pattern is slightly flatter, without the Eu anomaly that characterizes the metagranite-granodiorite (Figure 5-3). Interestingly, the metagranodiorite shows a trace element composition that is strikingly similar to that of the fine-grained rock of inferred volcanic origin, as described in the preceding section. Considering their spatial association, it seems reasonable to conclude that they are co-genetic.

5.2.3 Muscovite-rich, ductile deformation zone

Sample: *thin-section 400.96–401.04.*

The sample is from an interval of intense muscovitization between 394.5 and 401.4 m in KFM04A. Microscopic examination reveals that the rock mainly is composed of strained quartz and thin, booklet-shaped crystals of muscovite, with subordinate amounts of plagioclase and biotite. K-feldspar is notably absent. The distinct deformational fabric is marked of thin streaks of euhedral muscovite, intergrown with minor biotite. The general grain-size of the rock ranges up to 1.2 mm. The accessory minerals include sphene, zircon, epidote and unidentifiable opaque (< 20 μm in size). The rock appears, moreover, virtually unaffected by retrograde alteration.

The principal purpose of this sample was to identify relict metamorphic features that hopefully would provide insights in the protolith issue. However, complete metamorphic recrystallisation and suspected alkali metasomatism have rendered the recognition of the protolith more or less impossible.

5.3 The two facies of metagranite-granodiorite (101057) in KFM05A

Samples: *thin-sections 152.66–152.70, 272.11–272.15, 285.74–285.81 and 299.19–299.23 m and whole-rock geochemical samples 152.46–152.66, 271.90–272.11 and 298.82–299.02 m.*

In addition to the prevalent medium-grained metagranite-granodiorite, KFM05A includes a second, fine- to finely medium-grained variety. Except for the grain-size, there are no obvious differences between the two rock varieties. They are separated by a sharp, intrusive contact with an orientation of 163°/56°, at a borehole length of 285.8 m /Petersson et al. 2004b/. The fine- to finely medium-grained variety occurs in the upper part of the borehole, west of the contact. It has neither been distinguished in any other boreholes nor in outcrops visited during the bedrock mapping cf /Bergman et al. 2004/.

Microscopic examination reveals that the actual grain-size of fine to finely medium-grained variety is 0.1–1.3 mm with a few, elongated quartz grains ranging up to almost 5 mm in length. The general grain-size in the medium-grained variety is, on the other hand, up to 2 mm, with a few quartz grains that exceed 5 mm in length. The contact between the two facies are sharp intrusive also at a microscopic scale, and none of the rocks display any textural or mineralogical contact phenomena. Both facies have granular textures with irregular grain-boundaries. Also the textural character of individual minerals appears to be identical. However, with reservation for the low number of samples, there are consistent differences in the modal data for the two varieties. Biotite, which is the prime ferromagnesian mineral in these rocks, constitutes 3.4 and 3.8 vol. % of the total mode in the fine- to finely medium-grained variety. This is well within the range given by /Stephens et al. 2003; Petersson et al. 2004c/ for the medium-grained metagranite-granodiorite in the area cf /Stephens et al. 2003/, but it is far less than in the adjacent medium-grained variety that has a content of 6.8 vol. %. In the QAP diagram, the medium-grained variety plots in the granodiorite field, whereas samples of the more fine-grained variety plot in the monzogranite field (Figure 5-1). However, the actual spread within the group is small and all three analyses plot close to the boundary between the two fields.

The Q-P classification diagram gives a similar tight grouping at the boundary between the adamelite and granodiorite field (Figure 5-2). Neither the trace element analyses are diagnostic for separation. The patterns within a spider diagram are almost identical, with an enrichment of LIL relative to HFS elements (Figure 5-4). Moreover, they show all fractionated REE patterns, with pronounced Eu anomalies. There is, however, a rather large spread in the heavy REE, though the two extremes are samples of the more fine-grained variety. Based on the petrographic and geochemical similarity between the rock facies, we conclude that they originated as different surges of a single magma.

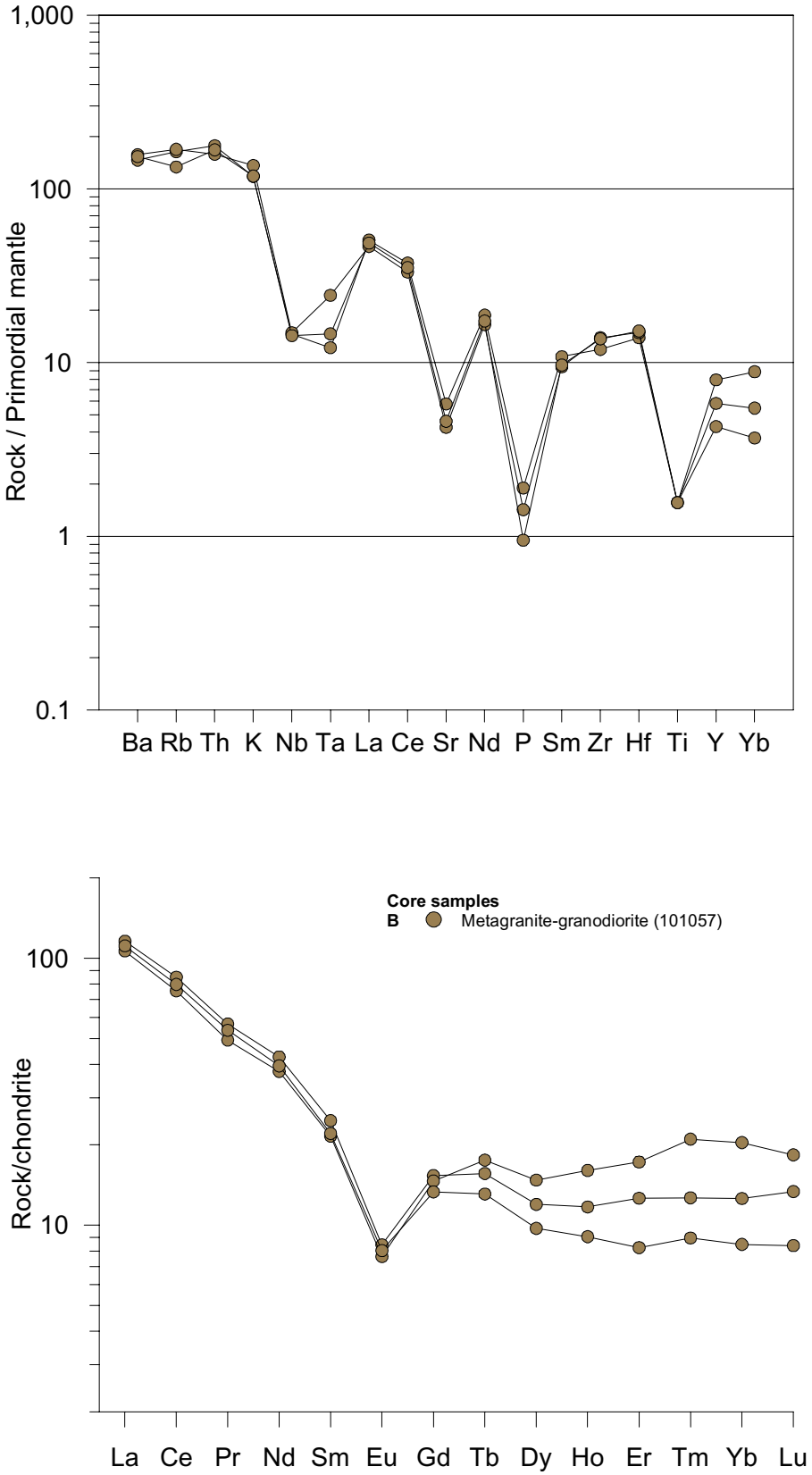

Figure 5-4. *Trace element variation diagrams for the two facies of metagranite-granodiorite in KFM05A. The upper diagram shows the relationships between large ion lithophile (LIL) and high field strength (HFS) elements normalized to the composition of the primordial mantle, whereas the lower diagram shows the rare earth element abundances normalized to chondritic meteorite values. Primordial mantle values of 92.000 for P (Sun, 1980) and 0.481 for Yb; all other after /McDonough et al. 1992/. Normalization factors for chondrite from /Boynton, 1984/.*

5.4 The whitened alteration rock in KFM06A and outcrops NE of the candidate area

Samples of the whitened alteration rock: *thin-sections 757.48–757.52, 818.33–818.36, 850.79–850.82 and 937.95–937.99 m and whole-rock geochemical sample 756.82–727.02, 818.42–818.62, 850.59–850.79 and 937.75–937.95 m. Outcrop samples: PFM001224B, PFM001229B, PFM001627A and PFM005197A.*

Samples of the unaltered equivalence: *thin-section 636.34–636.37 m and whole-rock geochemical sample 636.14–636.34 m. Outcrop sample: PFM001159B*

A more or less continuous occurrence of fine-grained whitish leucogranite extends from 755 to 966 m in borehole KFM06A. The white colour is imparted by the feldspars, though they have not the turbid or chalk white colour characteristic of albitized rock e.g. /Kamineni and Dugal, 1982; Baker, 1985; Petersson and Eliasson, 1997/. From macroscopic examination it is still obvious that the rock is the result of alteration. However, the alteration gives the impression of being pre- or possibly syn-metamorphic with no apparent relationship to existing brittle structures. The original magmatic textures are mostly masked or have been obliterated by the alteration. Based on the distribution of the ferromagnesian minerals it was inferred that the protolith comprises aplitic metagranite (rock code 101058) (thin-sections 850.79–850.82 and 937.95–937.99 m; whole-rock samples 850.59–850.79 and 937.75–937.95 m) with subordinate amounts of the medium-grained metagranite-granodiorite (rock code 101057) (thin-section 757.48–757.52 m; whole-rock sample 756.82–727.02 m). A possible candidate for the more fine-grained varieties is a fine-grained, distinctly foliated metagranite that occurs in a continuous length interval at 635–698 m in KFM05A (thin-section 636.34–636.37 m; whole-rock sample 636.14–636.34 m). A distinctly banded interval of the whitened rock is reminiscent of a volcanic protolith (thin-section: 818.33–818.36 m; whole-rock sample: 818.42–818.62 m). However, it has not been practically possible to separate this rock from the other fine-grained varieties, which probably originated as aplitic metagranite. The pre- or possibly syn-metamorphic origin of this alteration is further supported by the fact that some late veins and dykes of pegmatitic granite (101061) and fine- to finely-medium-grained metagranitoids (rock code 101051) appear unaffected by the alteration. This conclusion is, however, based on the well-preserved igneous texture rather than the feldspar characteristics.

Similar whitened rocks forms also minor occurrences at more shallow levels in KFM06A, and are ubiquitous as up to decimetre-wide rims around amphibolites. The contacts to the apparently unaffected wall rock are typically gradual over a few centimetres or some decimetre. Rocks affected by varying degrees of bleaching or whitening were also encountered during the field investigations in the area by the SGU. The vast majority of these occurrences are occurs within, or in close association with, the belt of aplitic metagranite that forms the northeastern limit of the tectonic lens (cf Figure 1-1).

All four thin-sections from the whitened rock interval in KFM06A reveal a granular texture with irregular grain-boundaries and a general grain-size of 0.1–0.8 mm (Figure 5-5). The most striking feature is the deficiency of K-feldspar relative to plagioclase. Only a few scattered K-feldspar grains were distinguished in each sample (see Figure 5-5), with a maximum of 0.6 vol. % in the sample from 937.95–937.99 m length. This is, however, somewhat illusory, since examination by SEM in back scatter mode reveals that minor K-feldspar frequently occurs peripherally in plagioclase crystals (Figure 5-6). Most of this K-feldspar is untwined and, therefore, almost impossible to distinguish optically from plagioclase. Although this means that the actual K-feldspar content is greatly underestimated, it will most certainly not affect the modal classification of the rocks, which consistently plot in the tonalite field on a QAP diagram (Figure 5-1). In addition, they are all rather quartz-rich relative to the apparently unaltered equivalents. The four outcrop samples of similar whitened rocks are also K-feldspar deficient, and plot in an array from the granodiorite to tonalite field in the QAP diagram.

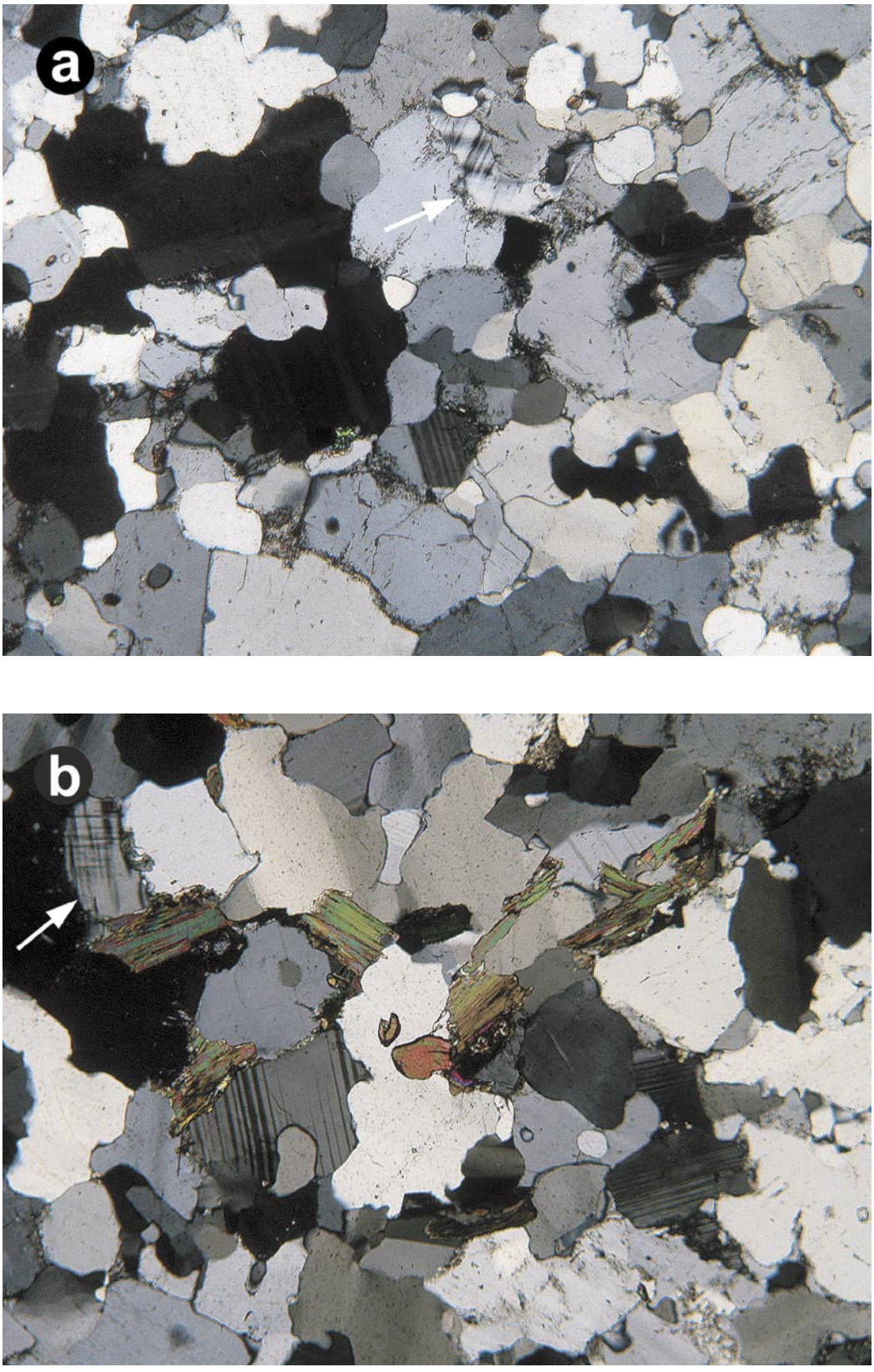

Figure 5-5. *Photomicrographs showing characteristic textural and mineralogical features of the whitened alteration rock in KFM06A. (a) Sample 850.79–850.82 m, and (b) sample 937.95–937.99 m. Note the K-feldspar grains marked by arrows. Fields of view are 2.9 x 2.2 mm.*

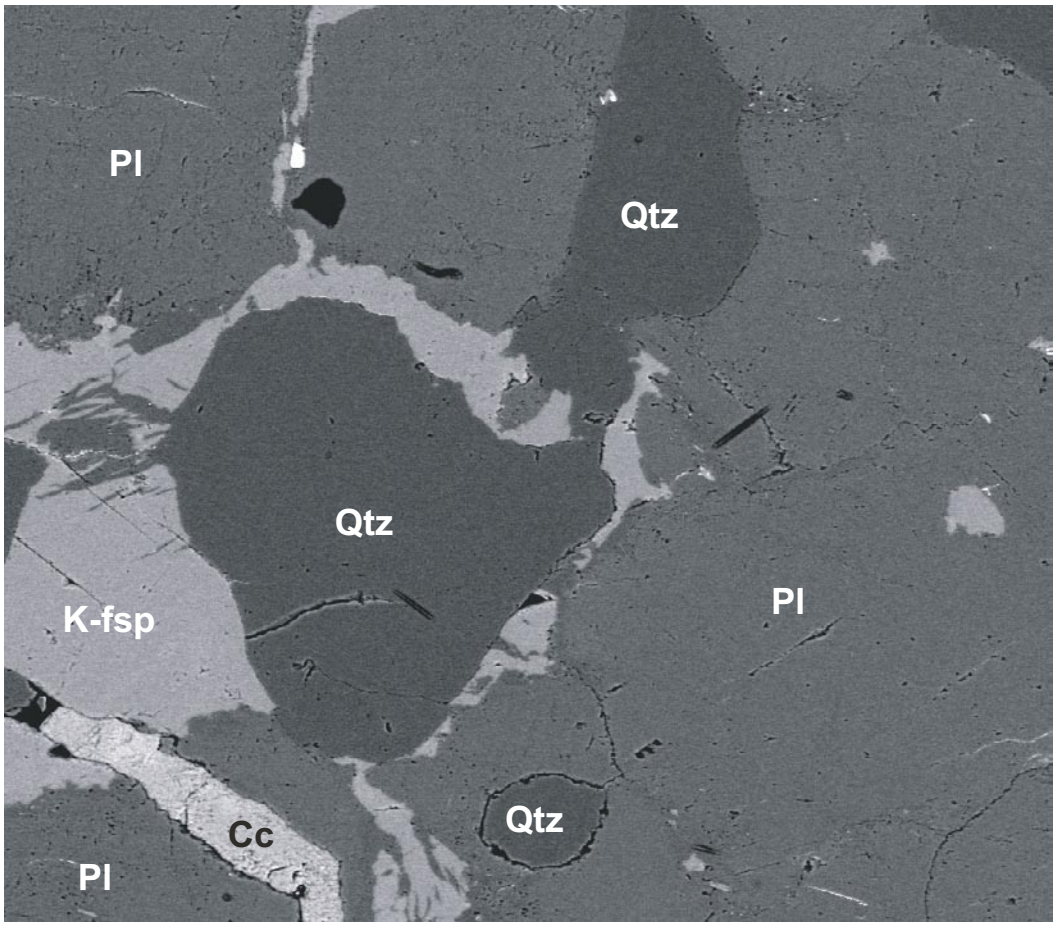

Figure 5-6. *BSE image showing the relationship between plagioclase (Pl), K-feldspar (K-fsp) and quartz (Qtz) in the whitened alteration rock. Also shown is a grain of calcite (Cc). Sample PFM5197A. Field of view is ~1.01 x 0.82 mm.*

The overall texture gives no definite clues to the protolith issue. However, the variability in the ferromagnesian mineralogy among the four samples suggests that the protoliths may differ. The ferromagnesian assemblage in the samples from 757.48–757.52 and 850.79–850.82 m comprises mainly epidote with subordinate hornblende (i.e. biotite is absent). The main ferromagnesian phases in the sample from 818.33–818.37 m are biotite and hornblende, whereas chloritized biotite prevails in the sample from 937.95–937.99 m, which moreover lacks hornblende. The accessory minerals are generally identical to those found in the apparently unaltered equivalences, and include sphene, magnetite, apatite, allanite, zircon and minor calcite. In addition, the sample from 818.33–818.37 m contains a few scattered grains of pyrite.

BSE examination of the feldspars in the both the whitened alteration rock and the unaltered equivalences (i.e. the medium-grained metagranite-granodiorite) show that they all are typically metamorphic without any distinguishable zonation or rimming (cf Figure 5-6). EDS analysis reveals, moreover, that the compositional variations are rather limited within individual samples, and the anorthite component ranges only by a few percentages in pristine plagioclase, unaffected by retrograde sericitization (see Appendix 4). The variations between the samples are, however, significant. Omitting an analysis from strongly sericitized domain (II:1 in sample 937.95–937.99), the plagioclase An content in all analyzed whitened alteration rocks ranges from 8.1 to 16.3 (n = 25) with an average of 12.5 ± 2.6 (1σ). Corresponding numbers for plagioclase from unaltered equivalences

of medium-grained metagranite-granodiorite range from 14.3 to 20.7 (n = 11) with an average of 18.0 ± 2.1 (1σ). Although there is an overlap in the ranges, it is obvious that plagioclases in the whitened alteration rock generally are more albite-rich than plagioclases in the unaltered equivalence (Figure 5-7). This becomes even more clear if the outcrop and core samples are compared internally. Also the composition of K-feldspar in the whitened alteration rock seems to differ from that in the medium-grained metagranite-granodiorite. Excepting one Or deficient analysis (III:1 in sample 757.48–757.52), the Or component in all analyzed K-feldspars from the whitened alteration rock ranges from 94.7 to 97.2 (n = 9), whereas the K-feldspars from the medium-grained metagranite-granodiorite display more constancy, and ranges from 94.2–94.9 (n = 4) (Figure 5-7).

The P-Q classification diagram confirms the quartz-rich and K-feldspar deficient nature of the whitened alteration rock; all samples are rather tightly clustered in the uppermost part of the tonalite field (Figure 5-2). Relative to the apparently unaltered equivalences, all samples have been highly Na enriched at the expense of K, whereas their Ca enrichment is more modest. This pattern is also reflected in the low content of trace elements that substitute for K, such as Ba and Rb (Figure 5-8). Other major elements that differs significantly are Fe and Ti, which is about half of that in the medium-grained metagranite-granodiorite samples. In the spider diagram of Figure 5-8, it is also evident that trace elements normally regarded as immobile are, enriched in the whitened alteration rock relative to the apparently unaltered equivalences. However, the Zr content is rather constant in all rocks plotted in Figure 5-8, and the most conspicuous enrichment is shown by Nb, Ta, Th and the REEs. Interestingly, this REE enrichment is systematic and the overall shape of the chondrite-normalized

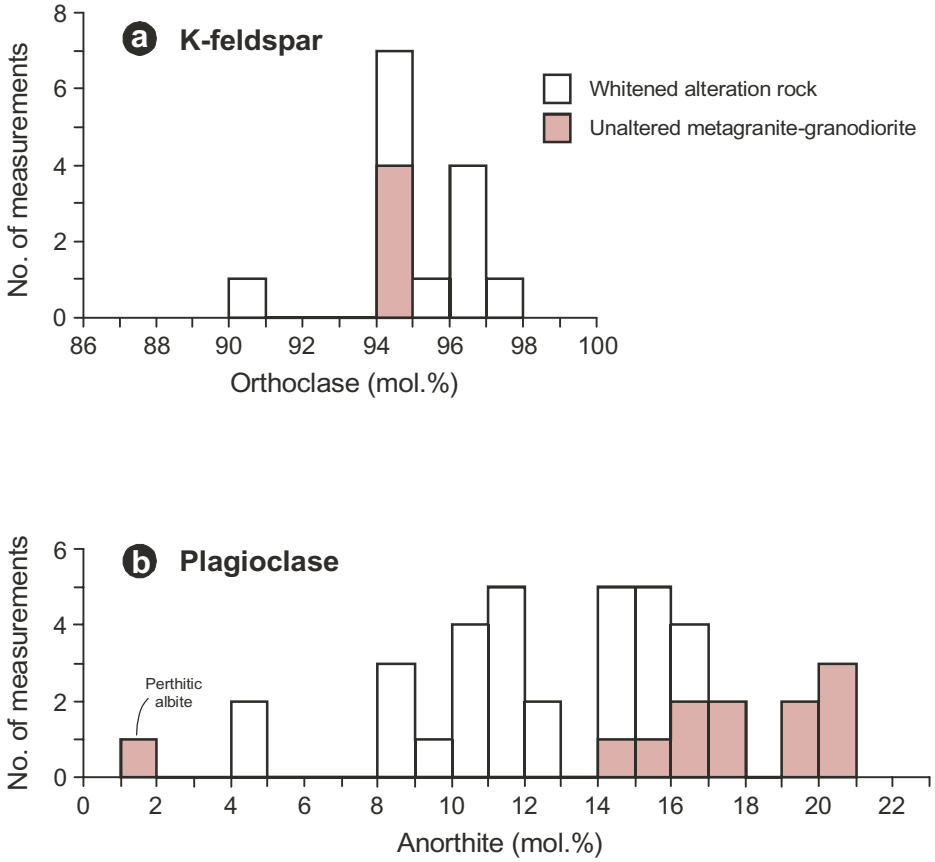

Figure 5-7. *Frequency histograms summarizing (a) the Or content in K-feldspar and (b) the An content in plagioclase for samples of both the whitened alteration rock and the medium-grained metagranite-granodiorite from outcrops and borehole KFM06A.*

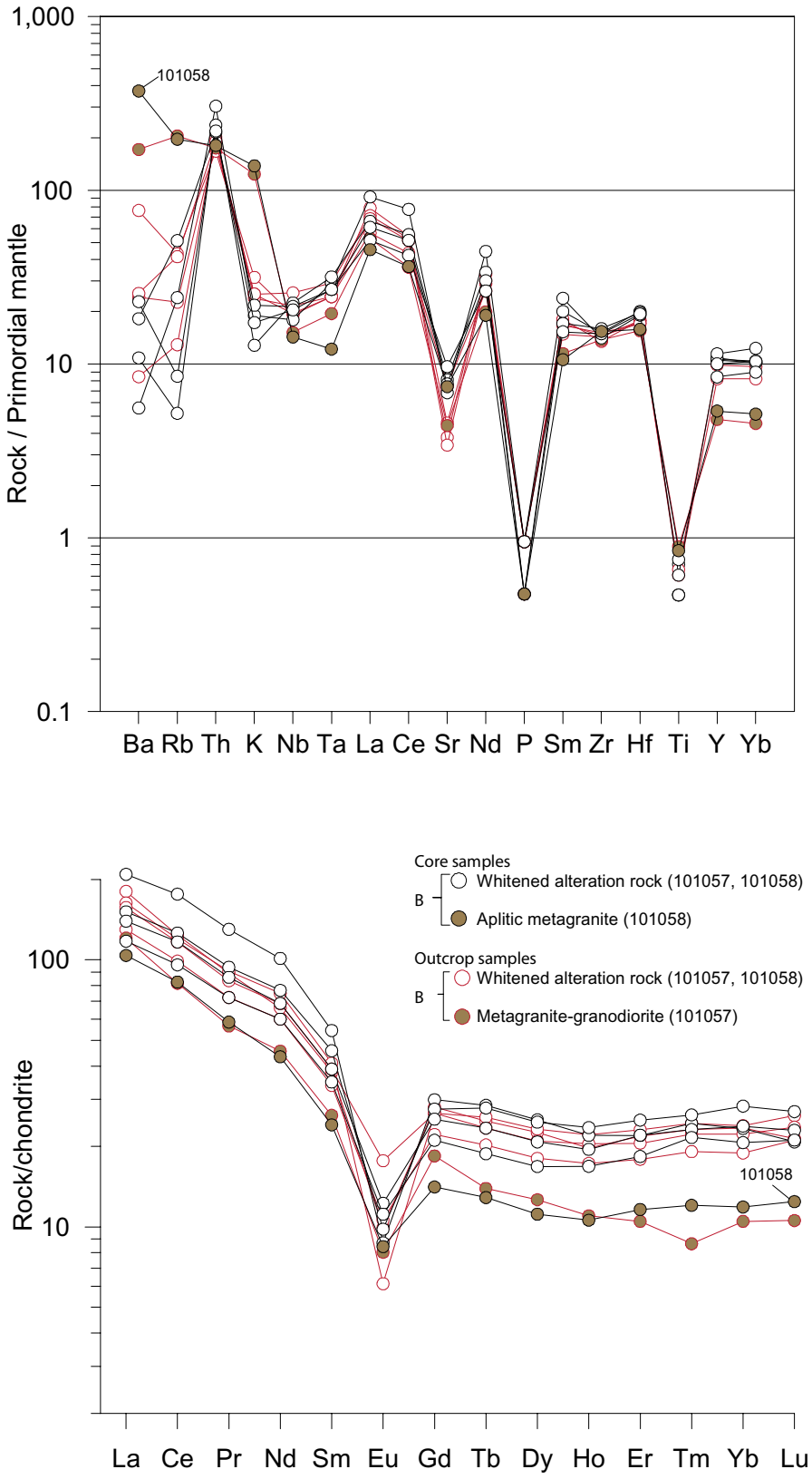

Figure 5-8. *Trace element variation diagrams for samples of both the whitened alteration rock and the medium-grained metagranite-granodiorite from outcrops and borehole KFM06A. The upper diagram shows the relationships between large ion lithophile (LIL) and high field strength (HFS) elements normalized to the composition of the primordial mantle, whereas the lower diagram shows the rare earth element abundances normalized to chondritic meteorite values. Primordial mantle values of 92.000 for P (Sun, 1980) and 0.481 for Yb; all other after /McDonough et al. 1992/. Normalization factors for chondrite from Boynton, 1984.*

patterns is virtually identical to that of the unaltered equivalences. Since the minerals that control the behaviour of the heavy and the light REEs are different, it is difficult to envisage a mechanism other than volume decease or mass loss which would give these patterns. Regarding the ore potential of this rock, it can be noted that three of the four analyses reveal a slight increase in the Au content relative to the medium-grained metagranite-granodiorite. However, the nearby, but unaltered aplitic metagranite (i.e. sample 636.14–636.34) shows an even greater enrichment. Gold enriched samples exhibit also a concomitant increase in their As content. From Appendix 3 it is evident that the Au and As content decrease towards depth in KFM06A. The most plausible explanation is that this enrichment is an artefact that resulted from contamination during the sample preparation; the sample prepared first got most contaminated.

Based on the general impression of the rock it was inferred already during the geological logging cf /Petersson et al. 2005/ that the alteration is pre- or possibly syn-metamorphic. This assumption is further supported by the fact that (1) there is no apparent relationship to existing brittle structures, and (2) some late veins and dykes appear unaffected by the alteration. The definite verification was achieved by the microscopic examination, which revealed a typical metamorphic texture with unzoned feldspars. The original alteration is hence masked or has been obliterated by the overprinting, amphibolite facies metamorphism. However, some general conclusions regarding the nature of the alteration can be given on the basis of the data given in the present study. The exceedingly low content of K-feldspar at the expense of plagioclase, as well as the low An content in the latter, suggest that the alteration is a form of albitization. Such a pervasive albitization would, however, give pure albite ($An_{0–5}$) e.g. /Kamineni and Dugal, 1982; Baker, 1985; Petersson and Eliasson, 1997/. A plausible interpretation is, therefore, that the original K-feldspar was almost completely replaced by albite in these rocks, and that the present mineralogy and composition of the feldspars is a result of metamorphic alkali redistribution at local scale. Another important finding, as indicated by both the variability and distribution of the ferromagnesian minerals among the samples, is that more than one rock type was affected by the alteration. Finally, the enrichment of typically immobile trace elements may suggest that the altered rock was subjected to volume reduction and/or mass loss.

5.5 Amphibolites and a possible sub-volcanic rock in KFM04A and KFM05A

Samples: *thin-sections 446.08–446.12, 737.61–737.65, 807.96–808.00 and 356.07–356.11 m and whole-rock geochemical samples 737.41–737.61 and 355.87–356.07 m.*

This group includes samples of three major amphibolite occurrences and of a fine-grained rock with intermediate composition, of inferred sub-volcanic origin. The amphibolites occur at 444.6–448.0 and 728.9–742.7 m in KFM04A and 348.9–362.1 m in KFM05A, whereas the fine-grained intermediate rock occurs at 806.4–808.4 m in KFM04A.

The three amphibolite occurrences are all texturally and mineralogically heterogeneous with highly variable grain-size and fabric. Sulphides are locally frequent and all occurrences appear to contain minor amounts of quartz. Macroscopic inspection of the occurrence at 444.6–448.0 m in KFM04A revealed also probable garnet and two generations of amphibole /Petersson et al. 2004a/. The fine-grained rock of inferred sub-volcanic origin is rather homogeneous, and the upper contact towards the medium-grained metagranite-granodiorite is gradual and rich in quartz segregations.

Modal analysis of two of the amphibolite samples reveals that they indeed are amphibolites, composed of more than 90 vol. % plagioclase and hornblende. Minor amounts of strained quartz were found in all three amphibolite samples. Other components found in minor to accessory amounts include sphene, epidote and apatite. Sample 446.08–446.12 from KFM04A contains also some biotite, often altered into chlorite and prehnite. However, the suspected garnet in this sample was shown to be discoloured plagioclase. Sample 737.61–737.65 from KFM04A contains, moreover, 2.0 vol. % K-feldspar. The sulphide assemblage comprises pyrite with subordinate chalcopyrite in all three samples.

The fine-grained rock of inferred sub-volcanic origin is rather massive with a granular texture and a general grain-size up to 0.8 mm. The fine-grained character is accentuated by a homogeneous distribution of the major mineral components (i.e. no aggregation). The sample was not analyzed modally, though the quartz content is estimated at 10–15 vol. %. Other major components are plagioclase and hornblende, which together constitute about 80–85 vol. % of the rock. Thus, the rock is a typical dacite according to the QAP classification diagram. In addition, it contains 5–7 vol. % biotite and accessory amounts of sphene, epidote, allanite, apatite and zircon.

Whole-rock geochemical analyses are available for two of the amphibolite samples. Similar to the modal analyses, they indicate that the rocks are of quartz dioritic to slightly gabbroic composition. The trace element compositions are generally in agreement with those of other amphibolites in the area cf /Stephens et al. 2003/, with negative spidergram anomalies for Nb and Ta, as well as slightly fractionated REE patterns (Figure 5-9).

5.6 Fine- to finely medium-grained metagranitoid in KFM05A

Samples: *thin-section 691.78–691.82 m and whole-rock geochemical sample 691.58–691.78 m.*

A major occurrence of fine- to finely medium-grained, equigranular metagranitoid of granodioritic to tonalitic composition (rock code 101051) occurs at 676–720 m length interval of KFM05A. The rock belongs hence to group C of /Stephens et al. 2003/, which is more or less coeval with the prevalent metagranite-granodiorite in the area cf /Page et al. 2004/. Accordingly, this intrusive shows gradual contact towards the surrounding, medium-grained metagranite-granodiorite, and it is often difficult to separate the two rocks from each other. Similar to other members of this group, it is locally somewhat porphyritic, with scattered K-feldspar megacrysts up to 2.5 cm in length. Significant amounts of garnet have also been identified in some sections.

The general grain-size of the rock is similar to that of the medium-grained metagranite-granodiorite and range up to 2.5 mm. However, minerals are more evenly distributed in the rock volume than in the metagranite-granodiorite in which they occur as polycrystalline domains. Rounded grains of plagioclase are typically coarsest, whereas quartz rarely exceeds 1.5 mm. All other phases are less than 1 mm in size. The major constituents are plagioclase (53.2 vol. %), strained quartz (24.8 vol. %), biotite (11.2 vol. %) and K-feldspar (6.4 vol. %), as well as some minor epidote (1.8 vol. %). In the QAP classification diagram it plots in the granodiorite field, but close to the nearby tonalite field (Figure 5-1). Retrograde metamorphic effects, such as serisitization of plagioclase and chloritization of biotite, are locally intense. The accessory assemblage includes hornblende (intimately associated with biotite), apatite, sphene (with rounded inclusions of Fe–Ti oxides, Figure 5-10), magnetite, zircon, allanite, prehnite, calcite and minor sulfides (pyrite, chalcopyrite and sphalerite). Garnet, which was expected from the macroscopic examination of the rock, is absent.

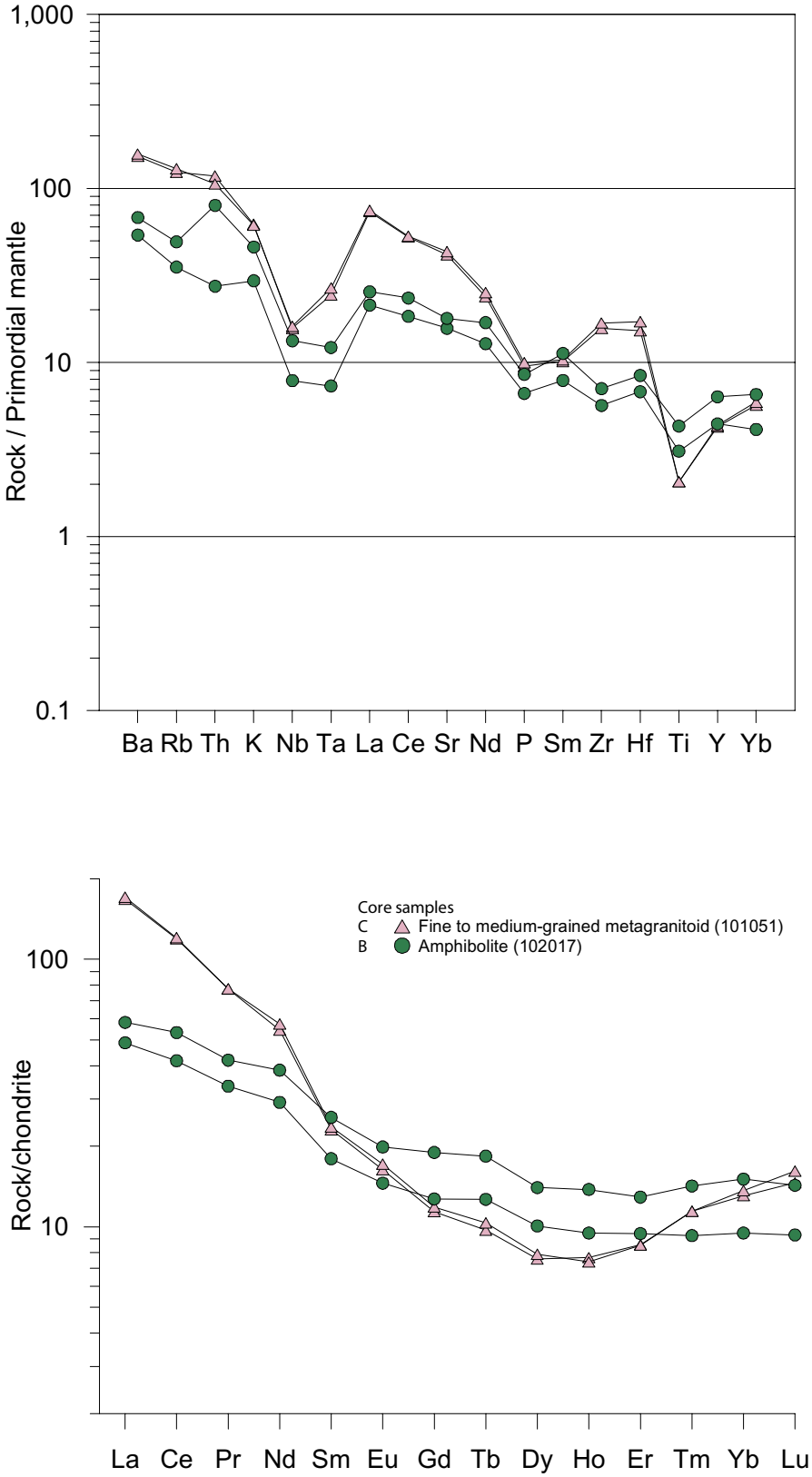

Figure 5-9. *Trace element variation diagrams for samples of two amphibolites and a fine- to finely medium-grained metagranitoid. The upper diagram shows the relationships between large ion lithophile (LIL) and high field strength (HFS) elements normalized to the composition of the primordial mantle, whereas the lower diagram shows the rare earth element abundances normalized to chondritic meteorite values. Primordial mantle values of 92.000 for P /Sun, 1980/ and 0.481 for Yb; all other after /McDonough et al. 1992/. Normalization factors for chondrite from /Boynton, 1984/.*

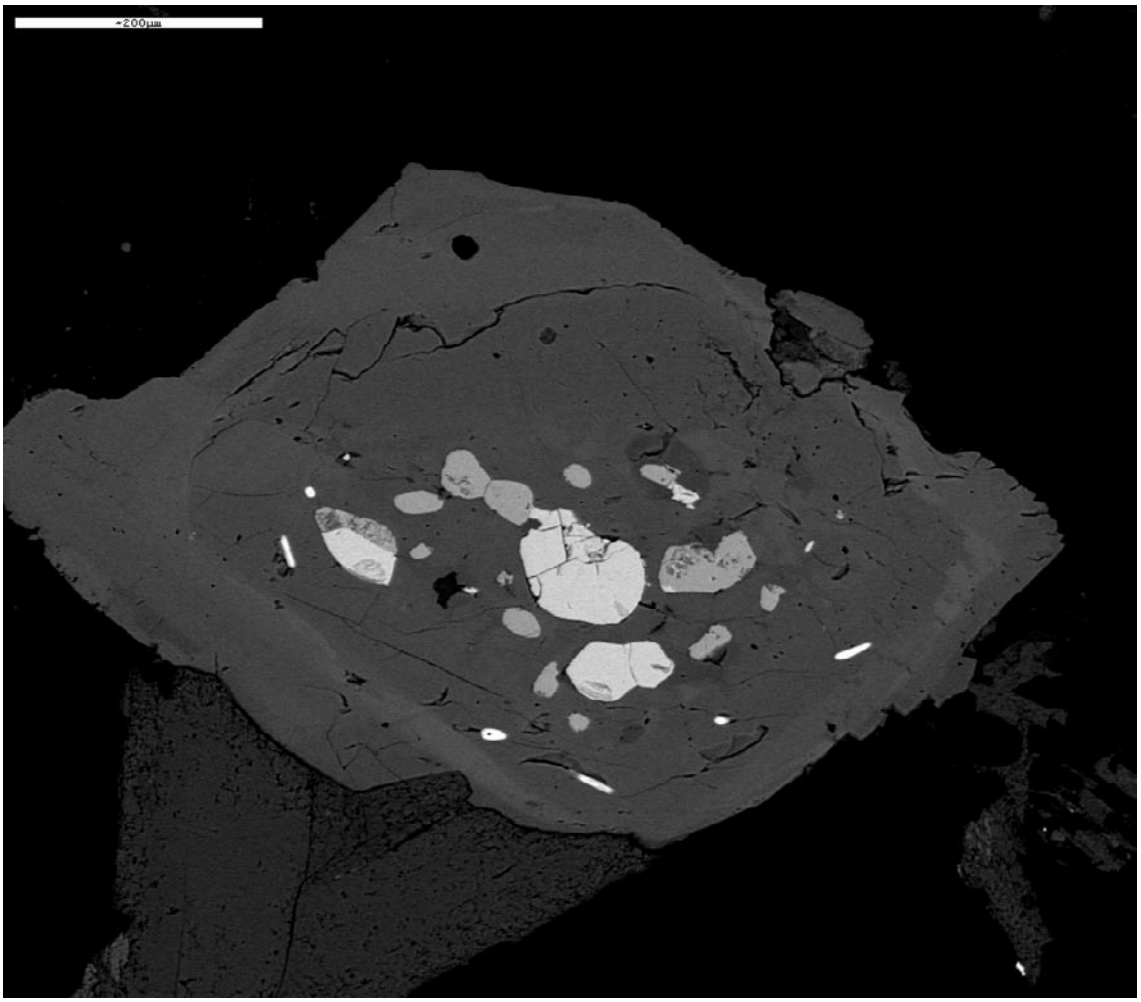

Figure 5-10. *BSE image of a subhedral sphene crystal with rounded inclusions of mainly magnetite (brightest) and ilmenite (slightly darker than magnetite). Field of view is ~0.92 x 0.8 mm.*

The rock shows a tonalitic composition on the Q-P classification diagram (Figure 5-2), in general agreement with the modal analysis. The trace element concentration, as illustrated in Figure 5-9, is typical for some of the tonalitic members of this rock group cf /Stephens et al. 2003; Petersson et al. 2004c/. Most strikingly it lacks the negative Sr anomaly in the spidergram and the Eu anomaly in the REE pattern. Such anomalies are typical for the vast majority of the granitoids in the area, and are mostly explained by plagioclase fractionation under reducing conditions. Another distinct feature is the concave-up spectrum for the heavy REE, commonly explained by fractional crystallization of hornblende, or alternatively, partial melting of an amphibolite, eclogite or garnet amphibolite source /Cullers and Graf, 1984/.

References

Baker J H, 1985. Rare earth and other trace element mobility accompanying albitization in a Proterozoic granite, W. Bergslagen, Sweden. Mineralogical Magazine, v. 49, p. 107–115.

Bergman T, Andersson J, Hermansson T, Zetterström Evins L, Albrecht L, Stephens M B, 2004. Forsmark site investigation. Bedrock mapping: Stage 2 (2003) – Bedrock data from outcrops and the basal parts of trenches and shallow boreholes through the Quarternary cover. SKB P-04-91. Svensk Kärnbränslehantering AB.

Boynton W V, 1984. Geochemistry of the rare earth elements: metiorite studies. In Henderson P (editor), Rare earth element geochemistry. Elsevier, pp. 63–114.

Cullers R L, Graf J L, 1984. Rare earth elements in igneous rocks of the continental crust: intermediate and silicic rocks – ore petrogenesis. In Henderson P (editor), Rare earth element geochemistry. Elsevier, pp. 275–316.

Debon F, LeFort P, 1983. A chemical–mineralogical classification of common plutonic rocks and associations. Transactions of the Royal Society of Edinburgh, Earth Sciences v. 73, p. 135–149.

Kamineni D C, Dugal J J B, 1982. A study of rock alteration in the Eye-Dashwa lakes pluton, Atikokan, northwestern Ontario, Canada. Chemical Geology, v. 36, p. 35–57.

McDonough W F, Sun S, Ringwood A E, Jagoutz E, Hofmann A W, 1992. K, Rb and Cs in the earth and moon and the evolution of the earth's mantle. Geochimica et Cosmochimica Acta, Ross Taylor Symposium volume.

Page L, Hermansson T, Söderlund P, Andersson J, Stephens M B, 2004. Forsmark site investigation. Bedrock mapping U-Pb, $^{40}Ar/^{39}Ar$ and (U-Th)/He geochronology. SKB P-04-126. Svensk Kärnbränslehantering AB.

Petersson J, Eliasson T, 1997. Mineral evolution and element mobility during episyenitization (dequartzification) and albitization in the postkinematic Bohus granite, southwest Sweden. Lithos, v. 42, p. 123–146.

Petersson J, Berglund J, Wängnerud A, Danielsson P, Stråhle A, 2004a. Forsmark site investigation. Boremap mapping of telescopic drilled borehole KFM04A. SKB P-04-115. Svensk Kärnbränslehantering AB.

Petersson J, Berglund J, Wängnerud A, Danielsson P, Stråhle A, 2004b. Forsmark site investigation. Boremap mapping of telescopic drilled borehole KFM05A. SKB P-04-295. Svensk Kärnbränslehantering AB.

Petersson J, Berglund J, Danielsson P, Wängnerud A, Tullborg E-L, Mattsson H, Thunehed H, Isaksson H, Lindroos H, 2004c. Forsmark site investigation. Petrography, geochemistry, petrophysics and fracture mineralogy of boreholes KFM01A, KFM02A and KFM03A+B. SKB P-04-103. Svensk Kärnbränslehantering AB.

Petersson J, Skogsmo G, Berglund J, Wängnerud A, Stråhle A, 2005. Forsmark site investigation. Boremap mapping of telescopic drilled borehole KFM06A and core drilled borehole KFM06B. SKB P-05-101. Svensk Kärnbränslehantering AB.

Sandström B, Savolainen M, Tullborg E-L, 2004. Forsmark site investigation. Fracture mineralogy: Results of fracture minerals and wall rock alteration in boreholes KFM01A, KFM02A, KFM03A and KFM03B. SKB P-04-149. Svensk Kärnbränslehantering AB.

SKB, 2004. Preliminary site description. Forsmark area – version 1.1. SKB R-04-15. Svensk Kärnbränslehantering AB.

Stephens M B, Lundqvist S, Bergman T, Andersson J, Ekström M, 2003. Forsmark site investigation. Bedrock mapping: Rock types, their petrographic and geochemical characteristics, and structural analysis of the bedrock based on Stage 1 (2002) surface data. SKB P-03-75. Svensk Kärnbränslehantering AB.

Stephens M B, Lundqvist S, Ekström M, Bergman T, 2005. Forsmark site investigation. Bedrock mapping. Petrographic and geochemical characteristics of rock types based on Stage 1 (2002) and Stage 2 (2003) surface data. SKB P-04-87. Svensk Kärnbränslehantering AB.

Streckeisen A, 1976. To each plutonic rock its proper name. Earth Science Reviews v. 12, p. 1–33.

Sun S S, 1980. Lead isotopic study of young volcanic rocks from mid-ocean ridges, ocean islands and island arcs. Philosophical Transactions of the Royal Society v. A297, p. 409–445.

Appendix 1

Descripion of thin-sections

KFM04A 117.70–117.74 m **Strongly foliated metagranodiorite (101056)**

Granular texture with irregular grain-boundaries and a distinct deformational fabric defined by elongated domains of plagioclase, strained quartz and streaks of ferromagnesian phases. The general grain-size is 0.1–1.0 mm. Plagioclase is typically coarsest, whereas quartz rarely exceeds 0.3 mm.

Mineral	*Vol. %*	*Textural character*
Quartz	15.6	Sub-grains with sutured contacts and undulose extinction.
K-feldspar	7.2	Typically tartan twinned.
Plagioclase	49.6	Generally slightly and locally strongly sericitized.
Biotite	2.2	The majority is chloritized.
Chlorite	4.2	Replaces biotite. More rarely as vermicular aggregates, < 50 µm in diameter.
Hornblende	16.2	
Epidote	3.0	Anhedral grains, < 0.3 mm, with very fine-scaled, symplectite texture.
Prehnite	+	Thin lenses in chlorite.
Sphene	1.8	Isolated, subhedral gains, < 0.2 mm in diameter.
Calcite	0.2	
Apatite	+	Stubby prisms, < 80 µm in diameter.
Opaque	+	Pyrite. Individual crystals < 0.1 mm in diameter.

KFM04A 124.56–124.60 m **Intermediate metavolcanitic rock (103076)**

Equigranular rock with granular texture and well-defined tectonic fabric. The general grain-size is 0.2–0.6 mm. This fine-grained character is accentuated by a strikingly homogeneous distribution of the major mineral components (i.e. no aggregation). A few irregular streaks of retrograde alteration marked by sercitization of plagioclase and weak chloritization of biotite.

Mineral	*Vol. %*	*Textural character*
Quartz	28.2	Sub-grains with sutured contacts and undulose extinction.
K-feldspar	0.4	Vague cross-hatched twinning.
Plagioclase	44.8	Locally affected by sericitization.
Biotite	25.6	Locally weakly chloritized.
Chlorite	0.4	Replaces biotite.
Epidote	+	Typically associated with biotite. Typically ~20 µm in diameter, with a few crystals reaching 80 µm.
Allanite	0.2	Isolated, strongly metamict grains, often surrounded by epidote.
Sphene	+	Irregular crystals, < 40 µm.
Apatite	0.4	Stubby prisms with a length/width ratio of ~4. Mostly < 40 µm in diameter, though a few crystals reach up to 80 µm.
Zircon	+	Rounded granis, < 20 µm.
Opaque	+	Mainly hematite found as inclusion in biotite. Individual crystals are less than < 20 µm in size.

KFM04A 186.65–186.70 m **Strongly foliated metagranite-granodiorite (101057)**

Granular texture with irregular grain-boundaries and a distinct deformational fabric defined by elongated domains of feldspars, strained quartz and the orientation of biotite. General grain-size up to about 1 mm, with a few grains ranging up to 1.5 mm. The rock is texturally very similar to that of thin-section 271.40–271.44 m.

Mineral	*Vol. %*	*Textural character*
Quartz	40.4	Sub-grains with sutured contacts and undulose extinction.
K-feldspar	19.8	Typically cross-hatched twinning and a few grains contain perthitic lamellae of albite.
Plagioclase	32.8	More or less strongly sericitized.
Biotite	5.2	Thin booklet-shaped crystals, rarely exceeding 0.5 mm in diameter. Some minor grains are chloritized.
Muscovite	+	
Chlorite	0.2	Replaces minor grains of biotite.
Epidote	1.0	Anhedral grains, < 0.2 mm, with very fine-scaled, symplectite texture.
Allanite	+	Strongly metamict grains, < 0.2 mm in length. Often epidote mantled.
Sphene	0.2	Anhedral granis, < 0.1 mm in length.
Opaque	+	Isolated, rounded grains of magnetite, < 150 µm in diameter. Also a minor grain of chalcopyrite.

KFM04A 271.40–271.44 m **Strongly foliated metagranite-granodiorite (101057)**

Granular texture with irregular grain-boundaries and a distinct deformational fabric defined by elongated domains of feldspars, strained quartz and thin streaks of biotite, as well as the orientation of individual biotite grains. The general grain-size is 0.1–1.5 mm. The rock is texturally very similar to that of thin-section 186.65–186.70 m.

Mineral	*Vol. %*	*Textural character*
Quartz	29.8	Sub-grains with sutured contacts and undulose extinction.
K-feldspar	21.0	Typically cross-hatched twinning, and locally, perthitic lamellae or ‘flames’ of albite.
Plagioclase	42.6	To a varying extent partially sericitized.
Biotite	5.8	Thin booklet-shaped crystals, none exceeding 0.5 mm in diameter. A few minor grains are chloritized.
Chlorite	+	Replaces minor grains of biotite.
Epidote	0.8	< 250 µm, with very fine-scaled, symplectite texture.
Allanite	+	Rounded, strongly metamict grains, < 150 µm in length. However, one epidote-mantled crystal reaches 0.7 mm in length.
Sphene	+	Occurs consistently as thin rims on magnetite.
Apatite	+	Stubby, rounded prisms, < 80 µm in diameter, and a length/width ratio of ~4.
Zircon	+	Rounded oscillary zoned crystals, < 80 µm in diameter.
Opaque	+	Isolated, irregular grains of magnetite, < 0.4 mm in diameter. Also some minor hematite.

KFM04A 400.96–401.04 m **Muscovite altered, ductile deformation zone (101057?)**

A rock mainly composed of muscovite and strained quartz, with subordinate amounts of plagioclase and biotite. K-feldspar is notably absent. Distinct deformational fabric marked by thin streaks of euhedral muscovite, intergrown with minor biotite. The accessory assemblage includes sphene, zircon, epidote and unidentifiable opaque. The general grain-size of the rock ranges between 0.1 and 1.2 mm.

Mineral	*Textural character*
Quartz	Sub-grains with sutured contacts and undulose extinction.
Plagioclase	Tends to be fresh and virtually unaffected by sericitization.
Biotite	Typically intergrown with muscovite.
Muscovite	Thin, booklet-shaped crystals, often exceeding 1 mm in length.
Epidote	
Sphene	Anhedral crystals, < 0.3 mm in length.
Zircon	Rounded crystals, < 20 µm in diameter.
Opaque	< 20 µm.

KFM04A 446.08–446.12 m **Sulphide- and quartz-bearing amphibolite (102017)**

Finely medium-grained rock with a general grain-size of 0.2–3.0 mm. The texture is granular and rather massive. Besides hornblende and plagioclase, comprising more than 90 vol. % of the mode, the rock contains minor amounts of strained quartz (individual grains up to 1.5 mm in size), biotite, sphene and various opaque phases, as well as accessory amounts of chlorite, epidote, prehnite, apatite and probable adularia.

Mineral	Textural character
Quartz	Sub-grains with sutured contacts and undulose extinction.
K-feldspar	Thin lenses of probable adularia in biotite.
Plagioclase	Generally slightly and locally, strongly sericitized.
Biotite	To a variable extent altered into chlorite and prehnite.
Chlorite	Alteration product of biotite.
Hornblende	Subhedral, often with scattered inclusions of sphene.
Epidote	< 0.3 mm, with very fine-scaled, symplectite texture.
Prehnite	Turgid lenses in chloritized biotite.
Sphene	Isolated, subhedral crystals, typically as inclusions in hornblende. Range in size up to ~1 mm. One crystal reaches 1.5 mm.
Apatite	Rounded crystals, < 150 µm in length.
Opaque	Pyrite and some minor grains of chalcopyrite.

KFM04A 737.61–737.65 m **Quartz-bearing amphibolite (102017)**

Granular texture with a weak deformational fabric defined by elongated, polycrystalline mineral domains and the orientation of hornblende crystals. The general grain-size is 0.1–1.5 mm.

Mineral	*Vol. %*	*Textural character*
Quartz	3.0	Sub-grains with sutured contacts and undulose extinction.
K-feldspar	2.0	Typically cross-hatched twinning.
Plagioclase	50.0	To a variable extent sericitized.
Hornblende	41.0	Thin booklet-shaped crystals, rarely exceeding 0.5 mm in diameter. Some minor grains are chloritized.
Epidote	1.6	Mainly as overgrowths on hornblende. Virtually all crystals exhibit a very fine-scaled, strongly symplectite texture.
Sphene	1.8	Mainly as tiny (< 0.1 mm), subhedral crystals hosted by hornblende. Also several coarser, sub- to euhedral crystals, ranging up to 1.5 mm in size.
Apatite	+	Stubby prisms, < 80 µm in diameter.
Opaque	0.6	< 0.3 mm in size. Pyrite and some minor grains of chalcopyrite.

KFM04A 807.96–808.00 m **Intermediate metavolcanic rock (103076)**

Rather massive plagioclase-hornblende dominated rock with an estimated quartz content of about 10–15 vol. %. The texture is granular with irregular grain-boundaries and a general grain-size is 0.1–0.8 mm. This fine-grained character is, moreover, accentuated by a homogeneous distribution of the major mineral components (i.e. no aggregation). The rock contains also about 5–7 vol. % biotite and ~1 vol. % sphene. The accessory minerals include apatite, epidote, zircon and allanite.

Mineral	*Textural character*
Quartz	Sub-grains with sutured contacts and undulose extinction.
Plagioclase	Locally slightly sericitized, though the majority is apparently unaffected by retrograde alteration.
Biotite	
Hornblende	
Epidote	< 0.1 mm.
Allanite	Epidote mantled and < 0.1 mm.
Sphene	Sub- to anhedral crystals, < 0.1 mm in size. A few crystals reach up to 0.3 mm in size.
Apatite	Stubby prisms, < 20 µm in diameter and with a length/width ratio of about 4.
Zircon	Rounded crystals, < 0.1 mm in size.

KFM05A 152.66–152.70 m **Metagranite-granodiorite (101057)**

Granular texture with irregular grain-boundaries and a faint tectonic fabric defined by thin elongated domains of strained quartz and thin streaks of biotite. The general grain-size is 0.1–1.3 mm, though a few elongated quartz grains may range up to almost 5 mm in length. Texturally and mineralogically almost identical with the rock of thin-section 272.11–272.15 m.

Mineral	*Vol. %*	*Textural character*
Quartz	39.2	Sub-grains with sutured contacts and undulose extinction.
K-feldspar	21.0	Typically cross-hatched twinning and locally, perthitic intergrowths comprising lamella or 'flames' of albite.
Plagioclase	35.0	Locally slightly sericitized.
Biotite	3.8	Booklet-shaped crystals.
Chlorite	0.2	Alteration product in minor grains of biotite.
Epidote	0.2	Subhedral crystals, < 250 µm in size and very fine-scaled, symplectite texture.
Allanite	0.2	Both small (< 150 µm), strongly metamict crystals and a few larger (< 1 mm) crystals mantled by epidote and less affected by metamictization.
Sphene	+	Consistently as overgrowths on magnetite.
Apatite	+	Stubby prisms, < 80 µm in diameter.
Zircon	+	Rounded, often oscillary zoned crystals, < 0.1 mm in diameter.
Opaque	0.4	Rounded grains of magnetite (< 0.7 mm), and some minor hematite enclosed in biotite and epidote.

KFM05A 272.11–272.15 m **Metagranite-granodiorite (101057)**

Rather massive rock, which is texturally and mineralogically almost identical to that of thin-section 152.66–152.70 m. Granular texture with irregular grain-boundaries. General grain-size up to 1.2 mm, with a few quartz grains ranging up to 3.5 mm in length.

Mineral	*Vol. %*	*Textural character*
Quartz	40.8	Sub-grains with sutured contacts and undulose extinction.
K-feldspar	24.4	Typically cross-hatched twinning.
Plagioclase	30.6	Locally slightly sericitized.
Biotite	3.4	Lobate, booklet-shaped crystals, rarely exceeding 0.8 mm in diameter.
Chlorite	0.2	Alteration product in minor grains of biotite.
Hornblende	0.2	Distinct green colour. Some grains up to 0.5 mm in size.
Epidote	0.2	Sub- to anhedral crystals, < 0.4 mm in size and very fine-scaled, symplectite texture.
Allanite	+	Both small (< 150 µm), strongly metamict crystals and a few larger (< 0.5 mm), isolated crystals mantled by epidote and less affected by metamictization.
Sphene	0.2	Both as overgrowths on magnetite and as isolated sub- to anhedral grains, < 0.8 mm in length.
Apatite	+	Stubby prisms, < 60 µm in diameter.
Zircon	+	Rounded, often oscillary zoned crystals, < 60 µm in diameter.
Opaque	+	Rounded grains of magnetite, < 0.4 mm in diameter.

KFM05A 299.19–299.23 m **Metagranite-granodiorite (101057)**

Granular texture with a distinct tectonic fabric defined by thin streaks of biotite and alternating domains of recrystallized feldspar and strained quartz. General grain-size up to 2 mm, with a few quartz crystals that exceed 5 mm in length.

Mineral	*Vol. %*	*Textural character*
Quartz	34.4	Sub-grains with sutured contacts and undulose extinction.
K-feldspar	18.6	Typically cross-hatched twinning, and some grains are rich in coarse, perthitic lamellae of albite.
Plagioclase	38.2	Generally slightly and locally, stongly sericitized.
Biotite	6.8	Booklet-shaped crystals, rarely exceeding 0.8 mm in diameter. Some minor grains are partially chloritized.
Chlorite	+	Alteration product in minor grains of biotite.
Hornblende	0.2	Distinct green colour, rarely reaching up to ~1 mm in size. Associated with biotite.
Epidote	0.6	Sub- to anhedral crystals that rarely reach up to 0.5 mm in size. Very fine-scaled, symplectite texture.
Allanite	0.2	Anhedral, metamict crystals, < 0.6 mm in length. Often with overgrowths of epidote.
Prehnite	0.8	Probably pumpellyite, which appears as thin lenses in biotite.
Sphene	0.2	Subhedral crystals, ranging up to 0.5 mm in size.
Apatite	+	A few stubby prisms, < 150 µm in diameter.
Zircon	+	Rounded crystals, < 120 µm in diameter. Often with a distinguishable oscillary zonation.

KFM05A 356.07–356.11 m **Amphibolite (102017)**

Rather equigranular with a general grain-size of 0.1–0.8 mm. Locally slightly coarser, where individual plagioclase crystals may reach up to 2.5 mm in length. The rock is more or less massive, with a vaguely defined mineral fabric.

Mineral	*Vol. %*	*Textural character*
Quartz	0.8	Undulose extinction.
Plagioclase	53.0	Generally slightly and locally, stongly sericitized.
Hornblende	42.6	
Epidote	0.6	Anhedral crystals,< 0.3 mm in size and with very fine-scaled, symplectite texture.
Sphene	2.0	Anhedral crystals, < 0.5 mm in size.
Apatite	1.0	Stubby prisms, < 70 µm in diameter and with a length/width ratio of 4–5.
Zircon	+	Rounded crystals, < 80 µm in diameter. Often with a vaguely distinguishable oscillary zonation.
Opaque	+	Irregular aggregates of pyrite, < 0.4 mm in size. Also a few minor (~20 µm) grains of chalcopyrite.

KFM05A 691.78–691.82 m **Metagranitoid, tonalitic (101051)**

Granular texture with irregular grain-boundaries and a general grain-size of 0.1–2.5 mm. Rounded grains of plagioclase are typically coarsest, whereas quartz rarely exceeds 1.5 mm in size. The rock exhibits, moreover, a faint tectonic fabric.

Mineral	*Vol. %*	*Textural character*
Quartz	24.8	Sub-grains with sutured contacts and undulose extinction.
K-feldspar	6.4	Typically cross-hatched twinning.
Plagioclase	53.2	To a variable extent sericitized. Also epidote is found in some of the most intensely altered grains.
Biotite	11.2	Booklet-shaped crystals, rarely exceeding 1 mm in diameter.
Chlorite	0.2	Alteration product in minor grains of biotite.
Hornblende	0.8	Distinct green colour. Often intimately associated with biotite.
Epidote	1.8	Subhedral crystals, < 0.5 mm in size and very fine-scaled, symplectite texture.
Allanite	+	Subhedral metamict crystals, < 0.4 mm. Some are overgrown by epidote.
Prehnite	+	One lenses in a chloritized biotite.
Sphene	0.4	Sub- to euhedral crystals, < 0.8 mm in length. Some crystals show a faint growth zoning.
Calcite	0.2	
Apatite	0.6	Stubby prisms, < 0.3 mm in diameter. Typically associated with aggregates of ferromagnesian phases.
Zircon	0.2	Rounded, often oscillary zoned crystals, < 0.1 mm in length.
Opaque	0.2	Mainly isolated grains of magnetite, rarely exceeding 0.2 mm in diameter. Also a few minor grains of pyrite, chalcopyrite and sphalerite. Rounded inclusions of magnetite and ilmenite in sphene.

KFM06A 636.34–636.37 m **Aplitic metagranite (101058)**

Granular texture that gives a massive impression. Irregular grain-boundaries and a general grain-size up to 0.6 mm, with a few, rounded K-feldspar crystals that reach 1 mm in diameter. This fine-grained character is, moreover, accentuated by a homogeneous distribution of the major mineral components (i.e. no aggregation).

Mineral	*Vol. % T.E.*	*Vol. % J.P.*	*Textural character*
Quartz	34.5	35.0	Sub-grains with sutured contacts and undulose extinction.
K-feldspar	30.7	22.6	Typically cross-hatched twinning and locally, perthitic intergrowths comprising lamella or ‘flames’ of albite.
Plagioclase	27.2	31.8	To a variable extent, partly sericitized.
Biotite	6.9	10.2	Thin booklet-shaped crystals, rarely exceeding 0.5 mm in width. Some minor grains are chloritized.
Chlorite	0.5	0.4	Alteration product in minor grains of biotite.
Epidote	+	+	Isolated, anhedral crystals, < 0.2 mm in size and very fine-scaled, symplectite texture.
Allanite	+	+	Sub- to euhedral metamict crystals, < 250 µm. Some are overgrown by epidote.
Sphene	+	+	Sub- to euhedral crystals, typically as inclusions in biotite.
Apatite	+	+	Stubby prisms, < 150 µm in diameter.
Zircon	+	+	Subhedral, often oscillary zoned crystals, < 60 µm in diameter.
Garnet	0.1	+	
Opaque	0.1	+	< 50 µm in diameter.

KFM06A 757.48–757.52 m **Albitized metagranite-granodiorite (101057)**

Granular texture with irregular grain-boundaries and a faint tectonic fabric defined by alternating domains of plagioclase and strained quartz. The texture is reminiscent of that shown by the metagranite-granodiorite (101057) elsewhere in the area. The general grain-size is 0.1–0.8 mm, though a few plagioclase grains may range up to 1.5 mm in size.

Mineral	*Vol. %*	*Textural character*
Quartz	39.0	Sub-grains with sutured contacts and undulose extinction.
K-feldspar	0.4	Anhedral and typically wedged between more rounded plagioclase crystals. Most grains display cross-hatched twinning.
Plagioclase	56.0	To a variable extent, partly sericitized.
Muscovite	0.2	
Hornblende	+	Distinct green colour. Occurs as scattered aggregates of anhedral grains, often associated with epidote.
Epidote	3.2	Anhedral crystals, < 0.5 mm in size and with very fine-scaled, symplectite texture. Typically associated with hornblende.
Allanite	+	Subhedral metamict crystals, < 250 µm. Some are overgrown by epidote.
Sphene	+	Sub- to euhedral crystals, < 150 µm in length, often with a vague, concentric zonation. Occurs both as clusters and as isolated crystals.
Calcite	0.2	
Apatie	+	Rounded crystals, < 60 µm in diameter.
Zircon	+	
Opaque	+	Anhedral and occasionally up to 0.5 mm in size. Mostly magnetite.

KFM06A 818.33–818.37 m **Albitized, aplitic metagranite (101058)**

Granular texture with irregular grain-boundaries and a general grain-size of 0.1–0.6 mm. The rock exhibits, moreover, a tectonic fabric defined by thin streaks of ferromagnesian material. However, individual minerals show no obvious preferred orientation.

Mineral	*Vol. %*	*Textural character*
Quartz	49.4	Sub-grains with sutured contacts and undulose extinction.
K-feldspar	+	Anhedral and typically wedged between more rounded plagioclase crystals. Most grains display cross-hatched twinning.
Plagioclase	43.2	Locally slightly sericitized, though the majority is apparently unaffected by retrograde alteration.
Biotite	3.2	Isolated, thin, booklet-shaped crystals, rarely exceeding 50 µm in width.
Chlorite	0.2	Alteration product in minor biotite grains.
Hornblende	2.4	Distinct green colour. Typically as isolated eu- to subhedral crystals, < 0.5 mm in size.
Epidote	1.0	Anhedral crystals, < 0.1 mm in size and with very fine-scaled, symplectite texture.
Allanite	+	Euhedral crystals, < 60 µm. Some are overgrown by epidote.
Prehnite	+	Both as turgid lenses in biotite and as isolated, sheaf-like aggregates.
Sphene	0.4	Subhedral crystals, < 60 µm in size.
Apatie	+	One single stubby prism, ~50 µm in diameter.
Zircon	0.2	
Opaque	+	Eu- to subhedral pyrite, < 50 µm in diameter.

KFM06A 850.79–850.82 m **Albitized, aplitic metagranite (101058)**

Granular texture that gives a massive impression. Irregular grain-boundaries with blebs of quartz. A general grain-size up to 0.8 mm and a few grains of quartz and plagioclase that reach 1.2 mm in diameter.

Mineral	*Vol. %*	*Textural character*
Quartz	50.0	Sub-grains with sutured contacts and undulose extinction.
K-feldspar	+	Anhedral and typically wedged along the edges of plagioclase crystals. Most grains display cross-hatched twinning.
Plagioclase	48.4	Locally slightly sericitized, though the majority is apparently unaffected by retrograde alteration.
Hornblende	+	Distinct green colour. Anhedral crystals, < 0.2 mm in size.
Epidote	1.0	Anhedral crystals with very fine-scaled, symplectite texture. Typically as overgrowths at allanite and magnetite.
Allanite	+	Euhedral crystals, < 60 µm in length. All crystals are overgrown by epidote.
Sphene	0.4	Subhedral crystals, < 0.1 mm in size.
Opaque	0.2	Rounded magnetite, < 0.3 mm in diameter.

KFM06A 937.95–937.99 m **Albitized, aplitic metagranite (101058)**

Granular texture with irregular grain-boundaries and a general grain-size between 0.1 and 1.0 mm. The rock is more or less massive.

Mineral	*Vol. %*	*Textural character*
Quartz	46.0	Sub-grains with sutured contacts and undulose extinction.
K-feldspar	0.6	Anhedral and typically wedged between more rounded plagioclase crystals. Most grains display cross-hatched twinning and a few, perthitic intergrowths comprising lamella of albite.
Plagioclase	50.2	Locally slightly sericitized, though the majority is apparently unaffected by retrograde alteration.
Biotite	1.2	Scattered aggregates, rarely exceeding 0.5 mm in size. Individual crystals are lobate in shape.
Chlorite	1.0	Strongly cleavage controlled alteration product in biotite.
Epidote	0.8	Anhedral crystals, < 0.2 mm in size and with very fine-scaled, symplectite texture.
Allanite	+	Subhedral crystals, < 350 µm in length. Some are overgrown by epidote.
Sphene	+	Subhedral crystals, < 60 µm in size.
Calcite	0.2	
Apatie	+	Isolated, rounded grains, < 150 µm in diameter.
Zircon	+	Euhedral crystals, < 50 µm in length.
Opaque	+	Anhedral crystals of mainly magnetite, < 0.1 mm in diameter.

Appendix 2

Modal analyses of thin-sections

	KFM04A					KFM05A				
Length	**117.70**	**124.56**	**186.65**	**271.40**	**737.61**	**152.66**	**272.11**	**299.19**	**356.07**	**691.78**
Rock type	Meta-granodiorite	Intermediate metavolcan.	Metagranite-granodiorite	Metagranite-granodiorite	Amphibolite	Metagranite-granodiorite	Metagranite-granodiorite	Metagranite-granodiorite	Amphibolite	Metagranitoid
Rock code	101056	103076	101057	101057	102017	101057	101057	101057	102017	101051
Rock group	**B**	**A**	**B**	**B**	**B**	**B**	**B**	**B**	**B**	**C**
Grain-size	0.1–1.0	0.2–0.6	0.1–1.5	0.1–1.5	0.1–1.5	0.1–1.3	0.1–1.2	0.1–2.0	0.1–0.8	0.1–2.5
Quartz	15.6	28.2	40.4	29.8	3.0	39.2	40.8	34.4	0.8	24.8
K-feldspar	7.2	0.4	19.8	21.0	2.0	21.0	24.4	18.6	–	6.4
Plagioclase[1]	49.6	44.8	32.8	42.6	50.0	35.0	30.6	38.2	53.0	53.2
Biotite	2.2	25.6	5.2	5.8	–	3.8	3.4	6.8	–	11.2
Muscovite	–	–	+	–	–	–	–	–	–	–
Chlorite	4.2	0.4	0.2	+	–	0.2	0.2	+	–	0.2
Hornblende	16.2	–	–	–	41.0	–	0.2	0.2	42.6	0.8
Epidote	3.0	+	1.0	0.8	1.6	0.2	0.2	0.6	0.6	1.8
Allanite	–	0.2	+	+	–	0.2	+	0.2	–	+
Prehnite	+	–	–	–	–	–	–	0.8	–	+
Sphene	1.8	+	0.2	+	1.8	+	0.2	0.2	2.0	0.4
Calcite	0.2	–	–	–	–	–	–	–	–	0.2
Apatite	+	0.4	–	+	+	+	+	+	1.0	0.6
Zircon	–	+	–	+	–	+	+	+	+	0.2
Opaque	+	+	0.4	+	0.6	0.4	+	–	+	0.2

+ = trace amounts.

[1] Including sericitized plagioclase.

	KFM06A					
Length	**636.34 *(T.E.)***	**636.34 *(J.P.)***	**757.48**	**818.33**	**850.79**	**937.95**
Rock type	Aplitic metagranite	Aplitic metagranite	Albitized meta-granite-granorite	Albitized, aplitic metagranite	Albitized, aplitic metagranite	Albitized, aplitic metagranite
Rock code	101058	101058	101057	101058	101058	101058
Rock group	**B**	**B**	**B**	**B**	**B**	**B**
Grain-size	0.1–0.6	0.1–0.6	0.1–0.8	0.1–0.6	0.1–0.8	0.1–1.0
Quartz	34.5	35.0	39.0	49.4	50.0	46.0
K-feldspar	30.7	22.6	0.4	+	+	0.6
Plagioclase [1]	27.2	31.8	56.0	43.2	48.4	50.2
Biotite	6.9	10.2		3.2		1.2
Muscovite			0.2			
Chlorite	0.5	0.4		0.2		1.0
Hornblende			+	2.4	+	
Epidote	+	+	3.2	1.0	1.0	0.8
Allanite	+	+	+	+	+	+
Prehnite				+		
Sphene	+	+	1.0	0.4	0.4	+
Calcite			0.2			0.2
Apatite	+	+	+	+		+
Zircon	+	+	+	0.2		+
Opaque	0.2 [2]	+	+	+	0.2	+

+ = trace amounts.

[1] Including sericitised plagioclase/albite.

[2] Including a single grain of garnet.

Appendix 3

Whole-rock geochemical analyses

	KFM04A					KFM05A					
Length	**116.51–116.70**	**124.60–124.80**	**186.57–186.80**	**271.64–271.84**	**737.41–737.61**	**152.46–152.66**	**271.90–272.10**	**298.82–299.02**	**355.87–356.07**	**691.58–691.78**	**Dupl. 691.58–691.78**
Rock type	Meta-granodiorite	Meta-volcanite	Metagranite-granodiorite	Metagranite-granodiorite	Amphibolite	Metagranite-granodiorite	Metagranite-granodiorite	Metagranite-granodiorite	Amphibolite	Metatonalite	Metatonalite
Rock code	101056	103076	101057	101057	102017	101057	101057	101057	101057	101051	101051
Rock group	**B**	**A**	**B**	**B**	**B**	**B**	**B**	**B**	**B**	**C**	**C**
SiO_2 (wt%)	62.45	67.20	75.23	75.41	55.29	76.33	76.30	74.93	53.70	69.56	69.55
TiO_2	0.62	0.49	0.17	0.18	0.92	0.18	0.16	0.18	0.66	0.44	0.44
Al_2O_3	15.24	13.96	12.62	12.42	13.82	12.35	12.32	12.83	15.43	14.71	14.64
Fe_2O_3	6.27	6.59	2.60	2.74	9.12	2.35	2.14	2.41	10.65	3.76	3.65
Cr_2O_3	0.001	< 0.001	< 0.001	< 0.001	0.018	< 0.001	< 0.001	< 0.001	0.009	< 0.001	< 0.001
MnO	0.10	0.14	0.03	0.04	0.15	0.03	0.03	0.04	0.17	0.04	0.04
MgO	2.65	2.35	0.32	0.30	6.36	0.21	0.16	0.30	5.08	1.05	1.04
CaO	5.36	1.53	1.35	1.47	8.68	1.39	1.26	1.72	8.72	3.49	3.52
Na_2O	3.48	4.52	3.25	3.11	3.36	3.30	3.28	3.39	3.60	4.06	4.21
K_2O	2.16	1.88	3.81	3.80	1.33	3.43	3.94	3.41	0.85	1.78	1.80
P_2O_5	0.17	0.14	0.04	0.05	0.18	0.02	0.03	0.04	0.14	0.21	0.20
LOI	1.3	1.1	0.5	0.4	0.6	0.2	0.3	0.7	0.7	0.6	0.6
TOT/C	0.02	0.02	0.03	< 0.01	0.02	0.23	0.01	0.01	0.02	0.01	0.01
TOT/S	0.03	0.01	0.02	0.01	0.15	< 0.01	< 0.01	0.01	0.09	0.06	0.07
SUM	99.80	99.90	99.92	99.92	99.84	99.80	99.93	99.95	99.71	99.70	99.70

	KFM04A					KFM05A					
Length	**116.51–116.70**	**124.60–124.80**	**186.57–186.80**	**271.64–271.84**	**737.41–737.61**	**152.46–152.66**	**271.90–272.10**	**298.82–299.02**	**355.87–356.07**	**691.58–691.78**	**Dupl. 691.58–691.78**
Be (ppm)	1	1	2	2	2	2	1	3	1	2	2
Sc	17	16	5	5	33	4	5	5	25	4	4
V	123	< 5	7	7	227	6	< 5	11	174	42	39
Co	16.0	5.9	2.5	2.3	30.3	1.9	1.5	2.7	32.5	7.0	7.7
Ni	4.6	1.5	2.8	2.3	13.1	2.8	2.1	2.3	8.0	6.3	6.4
Cu	12.4	11.6	11.1	65.6	44.8	8.3	7.0	7.0	22.8	30.3	29.1
Zn	44	92	28	27	23	23	21	26	37	49	50
Ga	19.2	18.6	16.5	16.1	19.3	14.1	14.8	15.8	18.7	21.7	21.3
As	1.1	0.6	0.7	0.7	0.6	< 0.5	0.7	0.5	0.5	< 0.5	0.6
Se	< 0.5	< 0.5	< 0.5	< 0.5	< 0.5	< 0.5	< 0.5	< 0.5	0.6	< 0.5	< 0.5
Rb	63.5	59.1	109.1	118.7	31.3	84.9	107.1	104.0	22.4	82.3	78.6
Sr	375.7	129.7	111.1	102.1	377.5	97.0	89.4	121.9	331.5	914.7	875.4
Y	25.9	26.9	28.8	27.3	28.9	19.5	36.2	26.5	20.2	19.8	19.4
Zr	165.5	141.7	136.2	150.9	79.2	153.5	155.9	133.4	63.4	188.8	175.7
Nb	8.4	8.1	12.2	11.7	9.5	10.2	10.6	10.4	5.6	11.5	11.2
Mo	1.3	0.6	1.8	0.7	0.5	1.3	0.7	0.7	0.8	0.6	0.8
Ag	< 0.1	< 0.1	< 0.1	0.1	< 0.1	< 0.1	< 0.1	< 0.1	< 0.1	< 0.1	< 0.1
Cd	0.1	< 0.1	< 0.1	0.1	< 0.1	< 0.1	< 0.1	< 0.1	< 0.1	< 0.1	< 0.1
Sn	< 1	2	2	2	3	2	2	3	2	3	3
Sb	0.1	0.1	0.1	0.1	0.1	0.1	0.1	0.1	< 0.1	0.1	0.1
Cs	0.8	4.1	1.0	1.5	0.3	0.3	0.6	1.1	0.6	0.9	0.9
Ba	618.8	673.2	1,187.9	1,080.2	474.5	1,072.8	1,099.9	1,023.2	376.7	1,101.5	1,068.1
Hf	5.2	4.4	4.3	4.5	2.6	4.7	4.6	4.3	2.1	5.3	4.7
Ta	0.5	0.5	0.8	0.5	0.5	0.6	1.0	0.5	0.3	1.0	1.0
W	0.4	0.5	0.6	0.1	0.8	0.4	0.4	0.3	< 0.1	< 0.1	< 0.1
Hg	0.02	< 0.01	< 0.01	< 0.01	< 0.01	0.01	< 0.01	< 0.01	< 0.01	< 0.01	< 0.01
Tl	0.1	0.3	0.2	0.3	< 0.1	0.2	0.2	0.2	0.1	0.3	0.3
Pb	2.5	4.9	3.2	3.4	1.6	3.8	4.0	5.2	1.3	2.5	2.5
Bi	0.3	0.1	0.2	0.2	0.1	0.2	< 0.1	< 0.1	0.1	0.1	0.1
Th	6.3	8.5	15.6	15.9	6.7	14.1	13.3	14.9	2.3	8.9	9.9
U	3.0	3.7	5.9	5.1	2.6	5.2	4.3	3.9	1.4	2.6	2.9
La	26.3	28.1	37.5	39.3	18.0	34.5	33.0	35.9	15.1	52.9	52.0
Ce	56.2	57.2	71.6	73.8	43.0	64.5	60.9	68.6	33.7	97.3	96.3
Pr	6.35	6.50	7.23	7.62	5.12	6.55	6.02	6.92	4.09	9.46	9.45
Nd	27.2	26.3	27.2	28.4	23.1	23.6	22.6	25.6	17.5	34.4	32.6
Sm	5.3	5.2	5.1	5.2	5.0	4.3	4.2	4.8	3.5	4.6	4.5
Eu	1.40	1.42	0.70	0.66	1.46	0.59	0.56	0.62	1.07	1.26	1.20
Gd	4.61	4.68	4.36	4.23	4.91	3.45	3.79	3.97	3.29	3.07	2.95
Tb	0.86	0.78	0.80	0.77	0.87	0.62	0.83	0.74	0.60	0.49	0.46
Dy	4.14	4.18	4.33	4.20	4.51	3.13	4.75	3.85	3.24	2.54	2.44
Ho	0.86	0.95	1.04	0.92	0.99	0.65	1.15	0.84	0.68	0.53	0.55
Er	2.48	2.66	2.83	2.64	2.71	1.73	3.62	2.65	1.98	1.79	1.80
Tm	0.39	0.43	0.50	0.42	0.46	0.29	0.68	0.41	0.30	0.37	0.37
Yb	2.54	2.80	3.24	2.76	3.15	1.77	4.26	2.63	1.98	2.85	2.73
Lu	0.38	0.42	0.52	0.42	0.46	0.27	0.59	0.43	0.30	0.52	0.47
Au (ppb)	3.5	1.4	0.9	1.1	< 0.5	2.6	1.4	1.1	0.6	1.0	1.0

	KFM06A					Standard	
Length	**636.14–636.34**	**756.82–757.02**	**818.42–818.62**	**850.59–850.79**	**937.75–937.95**	**SO-17/CBS**	
Rock type	Aplitic metagranite	Albitized meta-granite-granod.	Albitized, aplitic metagranite	Albitized, aplitic metagranite	Albitized, aplitic metagranite		
Rock code	101058	101057	101058	101058	101058		
Rock group	**B**	**B**	**B**	**B**	**B**		
SiO_2 (wt%)	75.97	76.68	76.81	78.04	78.29	61.70	61.66
TiO_2	0.18	0.16	0.13	0.10	0.10	0.57	0.60
Al_2O_3	12.31	13.16	12.74	12.65	12.40	13.74	13.83
Fe_2O_3	2.03	1.01	1.25	1.07	1.49	5.79	5.84
Cr_2O_3	< 0.001	0.001	< 0.001	< 0.001	< 0.001	0.447	0.452
MnO	0.03	0.02	0.01	0.01	0.03	0.53	0.53
MgO	0.63	0.24	0.81	0.03	0.13	2.42	2.35
CaO	0.99	2.40	1.74	2.14	1.85	4.60	4.68
Na_2O	3.10	5.29	5.34	5.07	4.95	4.05	4.14
K_2O	3.99	0.50	0.63	0.37	0.55	1.41	1.42
P_2O_5	0.01	0.02	< 0.01	0.01	0.02	0.98	0.98
LOI	0.4	0.5	0.5	0.5	0.1	3.5	3.4
TOT/C	0.03	0.04	0.04	0.01	0.02	2.39	2.41
TOT/S	0.04	0.09	0.03	0.03	0.01	5.28	5.33
SUM	99.64	99.98	99.97	100.00	99.91	99.75	99.89
Be (ppm)	1	2	3	4	3	1	1
Sc	4	5	4	4	3	23	23
V	9	8	< 5	< 5	< 5	131	129
Co	2.7	2.2	1.0	1.2	1.0	18.4	19.2
Ni	3.3	4.1	2.7	2.6	3.3	24.2	25.1
Cu	55.7	52.8	28.4	23.2	12.9	125.4	125.8
Zn	44	16	19	44	17	144	147
Ga	12.9	15.8	15.5	15.6	17.2	19.7	19.2
As	174.6	69.2	92.0	32.4	10.1	21.1	21.0
Se	1.8	1.4	1.1	0.9	< 0.5	4.6	4.4
Rb	124.8	5.4	32.5	3.3	15.3	23.7	24.1
Sr	156.5	203.8	162.1	171.5	144.3	308.0	306.7
Y	24.4	38.4	45.6	52.1	49.3	27.9	26.8
Zr	172.5	167.3	179.0	168.8	158.3	356.1	358.1
Nb	10.2	14.6	15.3	16.0	12.8	25.9	24.5
Mo	0.5	0.9	0.7	0.5	0.7	11.7	12.0
Ag	0.2	0.1	0.1	0.1	< 0.1	0.3	0.3
Cd	0.2	0.1	< 0.1	0.3	< 0.1	6.3	5.9
Sn	4	4	8	5	4	11	11
Sb	1.3	0.7	0.6	0.5	0.2	3.4	3.3

	KFM06A					Standard	
Length	**636.14–636.34**	**756.82–757.02**	**818.42–818.62**	**850.59–850.79**	**937.75–937.95**	**SO-17/CBS**	
Cs	0.6	< 0.1	0.5	0.1	0.4	3.8	3.8
Ba	2,603.5	159.6	127.4	75.8	39.0	397.5	401.7
Hf	4.9	6.0	6.1	6.2	5.9	12.6	12.9
Ta	0.5	1.1	1.1	1.3	1.2	4.2	4.3
W	0.3	0.4	0.3	0.3	0.1	10.1	10.2
Hg	0.02	0.01	0.01	0.02	0.01	0.24	0.24
Tl	0.2	< 0.1	0.1	< 0.1	< 0.1	1.8	1.7
Pb	5.7	4.1	3.0	3.6	4.5	30.4	29.5
Bi	0.1	0.2	0.1	0.1	< 0.1	5.2	4.8
Th	15.2	18.4	18.1	19.9	25.6	12.0	11.5
U	4.4	5.7	5.9	7.6	3.4	11.9	11.6
La	32.2	36.4	43.3	46.9	64.8	10.6	9.9
Ce	66.7	77.4	94.3	101.8	142.3	24.2	24.1
Pr	7.13	8.81	10.49	11.44	15.86	2.96	3.11
Nd	26.0	36.0	41.2	46.1	60.7	13.9	13.4
Sm	4.7	6.8	7.6	8.9	10.6	3.2	3.4
Eu	0.62	0.82	0.90	0.72	0.64	1.08	1.06
Gd	3.65	5.46	6.55	7.15	7.75	3.95	3.62
Tb	0.61	0.89	1.11	1.32	1.35	0.72	0.67
Dy	3.59	5.42	6.70	7.94	8.10	4.28	4.16
Ho	0.76	1.21	1.40	1.69	1.58	0.97	0.93
Er	2.44	3.85	4.63	5.27	4.62	2.78	2.77
Tm	0.39	0.70	0.75	0.85	0.79	0.44	0.44
Yb	2.48	4.32	4.98	5.92	4.88	2.83	3.00
Lu	0.40	0.68	0.74	0.87	0.67	0.45	0.44
Au (ppb)	26.5	10.5	10.9	6.6	1.3	45.1	44.0

Appendix 4

EDS analyses of various feldspars

	KFM05A: 285.74–285.81					KFM05A: 299.19–299.23			
Point no.	**I:1**	**I:3**	**II:1**	**II:3**	**I:2**	**I:1**	**I:3**	**II:1**	**I:2**
Feldspar	Oligoclase	Oligoclase	Oligoclase	Oligoclase	Microcline	Oligoclase	Oligoclase	Oligoclase	Microcline
SiO_2	65.17	64.86	64.84	64.80	65.85	64.07	63.99	64.25	66.04
TiO_2	0.01	–	–	0.02	0.20	0.03	0.04	–	0.21
Al_2O_3	23.40	23.03	23.43	22.87	19.27	23.81	23.84	24.08	19.16
FeO	0.02	–	0.04	0.06	0.12	0.10	0.04	0.09	0.01
MgO	0.07	–	0.02	–	–	–	–	–	0.02
CaO	3.73	3.45	3.66	3.45	–	4.34	4.21	4.17	–
Na_2O	9.35	9.30	9.47	9.31	0.63	9.14	8.80	8.97	0.67
K_2O	0.15	0.14	0.17	0.07	16.36	0.28	0.18	0.24	16.43
Total	101.89	100.77	101.63	100.58	102.43	101.77	101.10	101.80	102.54
Number of ions on the basis of 8 O									
Si	2.82	2.83	2.82	2.84	2.99	2.79	2.79	2.79	2.99
Ti	–	–	–	–	0.01	–	–	–	0.01
Al	1.19	1.19	1.20	1.18	1.03	1.22	1.23	1.23	1.02
Fe^{2+}	–	–	–	–	–	–	–	–	–
Mg	–	–	–	–	–	–	–	–	–
Ca	0.17	0.16	0.17	0.16	–	0.20	0.20	0.19	–
Na	0.78	0.79	0.80	0.79	0.06	0.77	0.74	0.76	0.06
K	0.01	0.01	0.01	–	0.95	0.02	0.01	0.01	0.95
Ab	81.3	82.3	81.6	83.0	5.5	78.0	78.2	78.5	5.8
An	17.9	16.9	17.4	17.0	0.0	20.4	20.7	20.1	0.0
Or	0.8	0.8	1.0	0.0	94.5	1.6	1.1	1.4	94.2

	KFM06A: 757.48–757.52								
Point no.	**I:1**	**II:1**	**III:2**	**IV:1**	**IV:B:1**	**IV:B:3**	**III:1**	**II:2**	**IV:B:2**
Feldspar	Oligoclase	Oligoclase	Oligoclase	Oligoclase	Oligoclase	Oligoclase	Microcline	Microcline	Microcline
SiO_2	63.94	64.23	64.64	64.87	66.00	64.09	64.31	65.23	65.51
TiO_2	–	–	0.07	0.02	–	0.01	0.39	0.13	0.02
Al_2O_3	22.56	22.92	22.34	22.45	21.83	22.52	19.03	19.15	18.94
FeO	0.08	–	0.09	0.01	0.02	0.07	–	0.03	0.08
MgO	–	–	0.04	–	–	–	–	0.08	–
CaO	3.26	3.31	3.19	3.09	2.30	3.20	–	–	–
Na_2O	9.30	9.43	9.43	9.38	9.95	9.30	1.04	0.60	0.46
K_2O	0.18	0.06	0.14	0.06	0.05	0.18	15.31	16.37	16.44
Total	99.31	99.94	99.93	99.87	100.15	99.38	100.09	101.61	101.46
Number of ions on the basis of 8 O									
Si	2.84	2.83	2.85	2.85	2.90	2.85	2.97	2.98	2.99
Ti	–	–	–	–	–	–	0.01	–	–
Al	1.18	1.19	1.16	1.16	1.13	1.18	1.03	1.03	1.02
Fe^{2+}	–	–	–	–	–	–	–	–	–
Mg	–	–	–	–	–	–	–	–	–
Ca	0.16	0.16	0.15	0.15	0.11	0.15	–	–	–
Na	0.80	0.81	0.81	0.80	0.85	0.80	0.09	0.05	0.04
K	0.01	–	0.01	–	–	0.01	0.90	0.95	0.96
Ab	82.9	83.7	83.6	84.6	88.7	83.1	9.4	5.3	4.1
An	16.1	16.3	15.6	15.4	11.3	15.8	0.0	0.0	0.0
Or	1.1	0.0	0.8	0.0	0.0	1.1	90.6	94.7	95.9

	KFM06A: 937.95–937.99								
Point no.	**I:A:1**	**I:A:2**	**II:2**	**III:1**	**III:2**	**II:1**	**I:A:3**	**II:3**	**III:3**
Feldspar	Oligoclase	Oligoclase	Oligoclase	Oligoclase	Oligoclase	Albite	Microcline	Microcline	Microcline
SiO_2	65.48	65.05	64.37	63.82	64.11	68.16	66.13	65.13	65.10
TiO_2	–	–	–	–	0.02	–	0.08	0.05	0.06
Al_2O_3	22.58	22.42	22.27	22.20	21.95	20.60	19.26	18.97	19.03
FeO	0.05	0.08	0.08	0.02	0.04	0.02	0.05	0.03	–
MgO	0.07	–	0.01	–	0.02	0.23	–	0.04	–
CaO	3.00	3.02	3.04	2.96	2.93	0.91	–	–	–
Na_2O	9.39	9.61	9.33	9.27	9.48	10.97	0.42	0.60	0.38
K_2O	0.16	0.05	0.17	0.12	0.16	0.01	16.83	16.19	16.20
Total	100.74	100.23	99.27	98.38	98.72	100.90	102.78	101.00	100.76
Number of ions on the basis of 8 O									
Si	2.86	2.86	2.85	2.85	2.86	2.95	2.99	2.99	2.99
Ti	–	–	–	–	–	–	–	–	–
Al	1.16	1.16	1.16	1.17	1.15	1.05	1.03	1.03	1.03
Fe^{2+}	–	–	–	–	–	–	–	–	–
Mg	–	–	–	–	–	0.01	–	0.04	–
Ca	0.14	0.14	0.14	0.14	0.14	0.04	–	–	–
Na	0.79	0.82	0.80	0.80	0.82	0.92	0.04	0.05	0.03
K	0.01	–	0.01	0.01	0.01	–	0.97	0.95	0.95
Ab	84.2	85.2	83.9	84.4	84.6	95.6	3.7	5.3	3.4
An	14.9	14.8	15.1	14.9	14.5	4.4	0.0	0.0	0.0
Or	1.0	0.0	1.0	0.7	0.9	0.0	96.3	94.7	96.6

	PFM1159							PFM001224	
Point no.	**I:1**	**I:4**	**II:1**	**II:3**	**I:3**	**I:2**	**II:2**	**I:1**	**II:1**
Feldspar	Oligoclase	Oligoclase	Oligoclase	Oligoclase	Albite	Microcline	Microcline	Oligoclase	Oligoclase
SiO_2	62.40	64.80	62.58	64.04	68.40	65.62	63.90	65.89	66.16
TiO_2	0.09	0.03	–	0.01	0.02	0.22	0.31	0.02	–
Al_2O_3	23.15	22.91	23.03	22.08	19.90	19.27	18.98	21.75	21.77
FeO	0.04	0.04	0.08	0.08	0.03	0.03	0.04	0.06	0.06
MgO	0.03	0.03	0.04	–	–	0.11	0.06	0.11	–
CaO	3.96	3.13	3.89	2.88	0.23	–	–	2.13	2.07
Na_2O	8.97	9.63	8.96	9.48	10.66	0.57	0.60	9.95	10.04
K_2O	0.16	0.11	0.15	0.10	0.61	16.23	16.05	0.14	0.14
Total	98.78	100.69	98.72	98.65	99.85	102.05	99.94	100.04	100.24
Number of ions on the basis of 8 O									
Si	2.79	2.84	2.80	2.86	2.99	2.98	2.97	2.89	2.90
Ti	–	–	–	–	–	0.01	0.01	–	–
Al	1.22	1.18	1.22	1.16	1.03	1.03	1.04	1.13	1.12
Fe^{2+}	–	–	–	–	–	–	–	–	–
Mg	–	–	–	–	–	0.01	–	0.01	–
Ca	0.19	0.15	0.19	0.14	0.01	–	–	0.10	0.10
Na	0.78	0.82	0.78	0.82	0.90	0.05	0.05	0.85	0.85
K	0.01	0.01	0.01	0.01	0.03	0.94	0.95	0.01	0.01
Ab	79.6	84.2	80.0	85.1	95.3	5.1	5.4	88.7	89.0
An	19.4	15.1	19.2	14.3	1.1	0.0	0.0	10.5	10.1
Or	0.9	0.6	0.9	0.6	3.6	94.9	94.6	0.8	0.8

	PFM001224					PFM001229			
Point no.	**II:2**	**I:2**	**I:3**	**I:2**	**I:3**	**II:2**	**II:3**	**I:1**	**II:1**
Feldspar	Oligoclase	Albite	Microcline	Oligoclase	Oligoclase	Oligoclase	Oligoclase	Albite	Microcline
SiO_2	65.86	65.44	64.90	65.50	65.17	65.73	65.16	66.97	65.29
TiO_2	0.03	0.00	0.14	–	–	–	–	0.04	0.03
Al_2O_3	21.95	21.59	19.15	21.79	21.39	22.29	21.85	20.47	19.08
FeO	0.10	0.06	0.05	0.09	0.02	0.01	–	0.05	–
MgO	0.01	–	0.04	0.02	0.01	0.06	–	0.03	0.09
CaO	2.13	2.00	–	2.23	2.03	2.47	2.36	0.89	–
Na_2O	10.10	10.26	0.35	9.90	9.99	10.00	9.95	10.69	0.39
K_2O	0.09	0.17	16.32	0.09	0.08	0.04	0.07	0.03	16.45
Total	100.26	99.51	100.94	99.62	98.69	100.59	99.38	99.18	101.33
Number of ions on the basis of 8 O									
Si	2.89	2.89	2.98	2.89	2.90	2.87	2.88	2.95	2.99
Ti	–	–	–	–	–	–	–	–	–
Al	1.13	1.12	1.04	1.13	1.12	1.15	1.14	1.06	1.03
Fe^{2+}	–	–	–	–	–	–	–	–	–
Mg	–	–	–	–	–	–	–	–	0.01
Ca	0.10	0.09	–	0.11	0.10	0.12	0.11	0.04	–
Na	0.86	0.88	0.03	0.85	0.86	0.85	0.85	0.91	0.03
K	–	0.01	0.96	0.01	–	–	–	–	0.96
Ab	89.6	89.4	3.2	88.5	89.9	88.0	88.4	95.6	3.5
An	10.4	9.6	0.0	11.0	10.1	12.0	11.6	4.4	0.0
Or	0.0	1.0	96.8	0.6	0.0	0.0	0.0	0.0	96.5

	PFM001627					PFM005197		
Point no.	**I:1**	**I:3**	**II:1**	**I:2**	**II:2**	**I:2**	**I:3**	**I:4**
Feldspar	Oligoclase	Oligoclase	Oligoclase	Oligoclase	Albite	Oligoclase	Oligoclase	Oligoclase
SiO_2	65.23	66.10	66.14	65.64	65.27	66.32	66.56	66.68
TiO_2	–	–	0.04	0.03	–	0.01	–	0.02
Al_2O_3	21.11	21.42	21.26	19.12	18.72	22.07	22.38	22.48
FeO	0.08	0.15	0.01	0.10	0.05	0.08	0.12	0.02
MgO	–	0.09	–	0.08	0.05	–	0.02	–
CaO	1.76	1.62	1.73	–	–	2.46	2.39	2.57
Na_2O	10.15	10.09	10.11	0.58	0.31	9.98	9.95	9.80
K_2O	0.07	0.17	0.07	16.47	16.45	0.14	0.11	0.12
Total	98.42	99.64	99.36	102.02	100.85	101.06	101.53	101.69
Number of ions on the basis of 8 O								
Si	2.91	2.91	2.92	2.99	3.00	2.88	2.88	2.88
Ti	–	–	–	–	–	–	–	–
Al	1.11	1.11	1.10	1.03	1.01	1.13	1.14	1.14
Fe^{2+}	–	0.01	–	–	–	–	–	–
Mg	–	0.01	–	–	–	–	–	–
Ca	0.08	0.08	0.08	–	–	0.84	0.83	0.82
Na	0.88	0.86	0.86	0.05	0.03	0.11	0.11	0.12
K	–	0.01	–	0.96	0.97	0.01	0.01	0.01
Ab	91.2	90.9	91.4	5.1	2.8	87.3	87.8	86.7
An	8.8	8.1	8.6	0.0	0.0	11.9	11.6	12.6
Or	0.0	1.0	0.0	94.9	97.2	0.8	0.5	0.7